sciendo

Reports on Geodesy and Geoinformatics, 2024, Vol. 117, pp. 69–88

DOI: 10.2478/rgg-2024-0008
Received: 28 November 2023 / Accepted: 10 April 2024
Published online: 23 May 2024

ORIGINAL ARTICLE

Evaluation of 2D affine — hand-crafted detectors for feature-based TLS point cloud registration

Jakub Markiewicz [1*]

[1]Department of Photogrammetry, Remote Sensing and Spatial Information Systems, Faculty of Geodesy and Cartography, Warsaw University of Technology, Pl. Politechniki 1, 00-661, Warsaw, Poland

[*]jakub.markiewicz@pw.edu.pl

Abstract

The development of modern surveying methods, particularly, Terrestrial Laser Scanning (TLS), has found wide application in protecting and monitoring engineering and objects and sites of cultural heritage. For this reason, it is crucial that several factors affecting the correctness of point cloud registration are considered, including the correctness of the distribution of control points (both signalised and natural), the quality of the process, and robustness analysis. The aim of this article is to evaluate the quality and correctness of TLS registration based on point clouds converted to raster form (in spherical mapping) and hand-crafted detectors. The expanded Structure-from-Motion (SfM) was used to detect the tie points for TLS registration and reliability assessment. The results demonstrated that affine detectors are useful in detecting a high number of key points (increased for point detectors by 8–12 times and for blob detectors by about 10–24 times), improving the quality and TLS registration completeness. For the registration accuracy of point cloud on signalised check points, the lower values can be noted for maximum RMSE errors for blob affine detectors than detectors and larger values for corner detectors and affine detectors (not more than 4 mm in the extreme cases, typically 2 mm). The commonly-applied target-based registration method yields similar results (differences do not exceed – in extreme cases – 3.5 mm, typically less than 2 mm), proving that using affine detectors in the TLS registration process is and reasonable and can be recommended.

Key words: affine 2D hand-crafted detectors; cultural heritage; interiors; feature based matching; reliability assessment; TLS registration

1 Introduction

Terrestrial laser scanning, due to its versatility, the speed of data acquisition and the accuracy of shape mapping, is commonly used to register, maintain, safeguard, and monitor various engineering objects (Mukupa et al., 2016), structural health monitoring (Dong et al., 2018; Rashidi et al., 2020; Vacca et al., 2016; Wang et al., 2014), construction management (Bosché, 2010), three-dimensional (3D) model reconstruction (Lu-Xingchang and Liu-Xianlin, 2006), and, especially, the preservation of cultural heritage monuments (Abbate et al., 2019; Arif and Essa, 2017; Giżyńska et al., 2022; Muradov et al., 2022; Wojtkowska et al., 2021). When analysing and processing complex and large-scale objects, a comprehensive acquisition of all elements within a single dataset is practically unachievable, which is due to inherent blind spots, intricacies in the object structure, and various measurement errors, including the beam refraction at the edges effect, intensity variations, and the impact of incidence angles (Bae and Lichti, 2008; Boehler et al., 2003; Staiger, 2005; Tobiasz et al., 2019). Terrestrial Laser Scanning (TLS) data are obtained within the instrument's local coordinate system. Consequently, in scenarios involving a substantial number of scans, as specified for large-size and complex objects, it becomes imperative to register these scans within a defined reference system, which involves preparing the plan for the TLS positions to facilitate the registration. The effectiveness of the TLS position distribution significantly affects the methodology and workflow employed

to register point clouds. In literature, numerous investigations address the challenge of TLS point cloud registration, focusing on its efficiency and robustness (Cheng et al., 2018; Pomerleau et al., 2015; Salvi et al., 2007; Tam et al., 2013; Weinmann, 2016). These studies categorise the methods by two principal criteria: (1) the effectiveness and robustness of the process based on the volume of input data, and (2) pairwise or multi-view registration (Dong et al., 2018). The predominant method employed in these algorithms is the coarse-fine strategy (Guo et al., 2013; Pavlov et al., 2017), which involves two key steps: (1) an initial approximation of translation and rotation parameters (Xu et al., 2019), and (2) a subsequent fine registration carried out by such algorithms as the normal distribution transform (NDT) and its variants (Biber and Straßer, 2003; Das and Waslander, 2012; Takeuchi and Tsubouchi, 2006), or the Iterative Closest Points (ICP) algorithm and its variants (Das and Waslander, 2012; Tazir et al., 2019).

The selection and configuration of tie points in the TLS registration process make a pivotal assumption: in evaluating the potential utilisation of tie points in TLS registration, it is imperative to assess their significance in terms of accuracy and the identification, localisation, and mitigation of outliers that may manifest during adjustment. Identifying outliers in observations and datasets used in the adjustment process conforms with the framework of reliability theory, which relates to the number and distribution of redundant observations. The network must use redundant information to diagnose observations containing outlier(s) effectively. The greater amount of information concerning the geometry of the network, the higher the likelihood of detecting outlier observations. Similarly, regarding the distribution of the redundant observations within the network – the more uniform this distribution, the more robust our construction in terms of reliability (Hekimoglu et al., 2002; Łapiński, 2011; Nowak and Odziemczyk, 2018; Prószyński and Łapiński, 2018; Rofatto et al., 2018).

In this investigation, TLS point cloud registration methodology used point clouds transformed into the intensity raster (with a depth map) and affine detectors (the modified version of the commonly-used detectors that applied the raster affine transformation). The article aims to show the potential applications, together with their constraints, of the use of detectors and their affine variants in the automatic TLS point cloud registration. Affine detector Investigations presented in this article are a continuation of the work presented in Markiewicz et al. (2023), which proposed the TLS-SfM approach of TLS data registration for three affine detectors (AFAST, ASIFT and ASURF). The present research aims to highlight that the choice of detector or affine detector affects data registration completeness, computation time, and registration quality. This article presents the effectiveness of different blob (CenSurE, SIFT, SURF) and point (BRISK, FAST) detectors and the effect of the affinity (ABRISK, ACenSurE, AFAST, ASIFT, ASURF) into the stage of point detection with quality and robustness analysis, grounded in a reliability assessment.

The TLS-SfM results were compared with those obtained from the commonly used target-based method and ICP. The study shows that the proposed TLS point cloud registration method offers an advantage over the target-based method. This results in a higher number of more evenly distributed points and affects better outlier removal as per the reliability theory. In the case of the ICP method, usually based on point-to-point and point-to-plane methods, the point clouds' initial (approximate) orientation is required. Meeting this condition guarantees the correctness of the final point cloud registration. Crucially, in the TLS-SfM method, point cloud pre-registration is not required, as the extraction of tie points is used in a two-step manner through descriptor matching and geometrical verification, based on the Random Sample Consensus (RANSAC) algorithm (Fischler and Bolles, 1981).

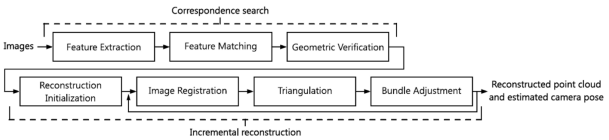

Figure 1. Incremental SfM methodology (Bianco et al., 2018)

This article presents the principles of 2D feature detection and description in Section 2. In Section 3, the used test sites and proposed TLS-SfM approach are presented. Section 4 examines the outcomes of the detector evaluations, and Section 5 concludes by presenting the advantages and drawbacks of employing various affine 2D detectors along with approaches for future work.

2 TLS point featured-based cloud registration

Presently, the Structure-from-Motion (SfM) method, which is a computer vision and photogrammetric technique, plays a pivotal role in image orientation and three-dimensional (3D) reconstruction of scenes or objects from two-dimensional (2D) image sequences. It aims to recover a scene's spatial arrangement and simultaneously estimate the camera exterior orientation parameters, intrinsic parameters, and the 3D structure of observed features.

The foundation of SfM lies in exploiting visual information from multiple images, especially by feature matching or, generally, image matching. It is used to determine the correspondence between two images or features of the same scene. The workflow of SfM can be divided into the correspondence search phase and the iterative reconstruction phase (Bianco et al., 2018; Markiewicz, 2016; Moussa, 2014; Urban and Weinmann, 2015). The correspondence search part involves extracting tie points using a detector and descriptor for feature extraction and feature matching, and, finally, using geometric verification for outlier removal. Detecting key points (using detectors) and determining tie points as a result of descriptor matching uses the so-called hand-crafted or learned-based methods. Hand-crafted features have for many years been used for feature detection or feature description. The key algorithms, for example: the Harris algorithm, FAST, or SIFT are based only on changes in gradients, grey degrees, corners, etc., detected only in the processed image. In contrast to hand-crafted methods, learned-based algorithms are based on trained deep Convolutional Neural Networks (CNNs) on learning sets based on a number of different reference rasters. The hand-crafted detectors and descriptors (referred to in the article as *detectors and descriptors*) used to determine the tie points are described in detail in subsection 2.2.

The Incremental reconstruction phase is based on the reconstruction initialisation, images registration, triangulation, and the bundle adjustment (Figure 1).

The commonly used SfM method is designed for image processing. Therefore, it is impossible to use this algorithm directly, and it is necessary to modify the input data and the Geometric Verification step. A detailed description of the modified TLS-SfM method is provided in Markiewicz et al. (2023), and how the above steps can be modified is explained in sections 2.1 and 2.2.

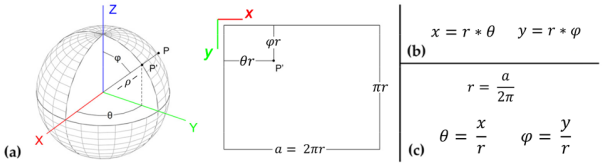

Figure 2. Relations between spherical coordinates and coordinates on spherical images. (a) Graphical representation of the relations between polar coordinates measured and the raster image in spherical projection, (b) formula for recalculation of polar coordinates to spherical projection of arbitrary radius *r*, and (c) formula for recalculation of *x*, *y* spherical projection onto polar coordinates (Markiewicz and Zawieska, 2019; Markiewicz et al., 2023)

2.1 The spherical image generation

To use SfM algorithms for TLS point cloud orientation, it is necessary to conduct the point cloud conversion into the spherical raster based on the cartographical equation (Figure 2b) (Markiewicz and Zawieska, 2019). Most TLSs are based on a panoramic architecture, and they directly measure three values: ρ – the distance from the object to the scanning position, θ – horizontal angle and φ – vertical (elevation) direction (Figure 2). An acquisition of this data is possible in two ways: by reading the data from native files using the Software Development Kit (SDK) or by converting it based on the convertible equations 1–3:

$$X = \rho \cos\theta \sin\varphi \quad (1)$$

$$Y = \rho \sin\theta \sin\varphi \quad (2)$$

$$Z = \rho \cos\varphi \quad (3)$$

The pixel coordinates of the generated raster correspond to the horizontal and vertical angle values (Figure 2a). The method of point cloud representation in spherical projection is widely used in the field. It is implemented in many commercial software tools. The main usefulness of this data representation method is the ability to use the raw data and generate a raster with the highest resolution without interpolating new values for pixel coordinates. Furthermore, generating an intensity raster at arbitrary resolutions is facilitated by transforming pixel values according to the formulas provided in Figure 2.

Intensity rasters prepared in this way enable detectors to extract the key points. Using the *x* and *y* coordinates of the detected points, it is possible to determine the coordinates of points based on depth maps and equations 1–3 or to interpolate them based on *X*, *Y*, and *Z* maps. In this way, it is possible to compute the *XYZ* points coordinates used in the final step of determining the 3D transformation parameters.

2.2 The theory of the 2D feature hand-crafted matching – the feature extraction, matching and images registration

In the SfM workflow, the first and most crucial step is feature detection (also called: extraction), which is used for feature extraction – to recognise in each image (image from a group of images) characteristic features (also called key points) such as lines (Canny, 1986), points (Harris and Stephens, 1988) or blobs (Lowe, 1999) based only on local characteristics of the intensity value.

The feature extraction part is performed on each image separately and based on the algorithms and methods which detect features invariant to image translation, scaling, and rotation, partially invariant to illumination changes, and robust to local geometric distortions such as SIFT (Bay et al., 2006; Harris and Stephens, 1988; Moussa, 2014; Tuytelaars and Mikolajczyk, 2007). Each detected feature is analysed for gradient change based on its nearest neighbour to assign unique features. Nowadays, corner detectors like FAST (Rosten and Drummond, 2006) and BRISK (Bay et al., 2006), as well as blob detectors such as SIFT (Lowe, 2004), SURF (Leutenegger et al., 2011), and CenSurE (Agrawal et al., 2008), are utilised for keypoint extraction. These detectors were used in this study for automatic point cloud registration.

The next step in SfM data processing involves describing the characteristic features based on gradient changes concerning their nearest neighbours. Various descriptors, such as SIFT, SURF, or DAISY, as documented in literature (Bay et al., 2006; Lowe, 2004; Tola et al., 2010), are available. The SIFT descriptor employed in this investigation is based on computing local image gradients within a specified scale surrounding the key point of interest. The descriptor's methodology involves an analysis of histograms constructed from 4×4 pixel neighbourhoods, each comprising 8 bins representing orientations. These histograms are generated from magnitudes and orientations sampled within a 16×16 region centred on the key point. For each histogram, a 4×4 subregion is sampled from the original neighbourhood. The magnitude and orientation of image gradients are computed around the key point location, with the key point's scale determining the image selection. To achieve orientation invariance, the descriptor coordinates and gradient orientations are rotationally adjusted relative to the key point orientation (Karwel and Markiewicz, 2022). The detailed description of the above-mentioned detectors and affine detectors can be found in the following publications: Yu and Morel (2011) and Markiewicz and Zawieska (2019).

Upon assigning descriptor features to the key points, identifying correspondences and overlapping images becomes feasible, thereby enabling the determination of tie points. This process unfolds in a two-stage fashion, encompassing (1) the initial identification of potential point pairs through descriptor matching, and (2) geometric verification, employing an iterative approach based on the RANSAC method, incorporating homography functions (Moisan and Stival, 2004).

Various strategies can be employed to compute matches between images effectively, for example, brute-force matching or approximate nearest-neighbour-based point matching. Although descriptor matching provides candidate tie points, there is no assurance that these correspond to 3D points in the scene, potentially incorporating outliers. Consequently, a geometrical verification becomes imperative to eliminate outliers, enhance the quality of tie points, and adjust the image's orientation.

With TLS point cloud registration, this process is improved. In the case of image processing, the coordinates of 2D points are used, and a homography model is determined. Using this for TLS point clouds, it is mandatory to determine the points' 3D coordinates and apply a 6-parameter transformation.

Bundle adjustment plays a critical role in geodesy and 3D reconstruction, constituting a central component of contemporary multiview geometry systems. Typically, at a final refinement stage, bundle adjustment approximates initial scene estimates and serves as a mechanism for mitigating drift in incremental reconstructions (Chen et al., 2019). This adjustment allows for the determination of the orientation of all images within a block while minimising reprojection and computing optimal camera calibration parameters in the self-calibration process. With TLS point cloud registration, the distance between point clouds is minimised, and, unlike with image processing, no self-calibration is performed.

Table 1. List of point clouds with parameters

Test Site name	Scanner type	Angular resolution Horizontal	Angular resolution Vertical	Point scan resolution	No. scans	Avg. number of points per scan
I – Basement in the Royal Castle	Z+F 5006	360°	320°	6.3 mm/10 m	4	43,120,284
II – Basement in the Royal Castle	Z+F 5006	360°	320°	6.3 mm/10 m	6	42,145,054
III - "The Queen's Bedroom," in the Museum of King Jan III's Palace at Wilanów	Z+F 5003	1 scan-360° 5 scan-90°	1 scan-320° 1 scan-180°	3.2 mm/10 m	6	1 scan-42,308,262 5 scan-126,913,021
IV - "The Chamber with a Parrot," in the Museum of King Jan III's Palace at Wilanów	Z+F 5006	360°	320°	6.3 mm/10 m	4	40,320,455
V – "The office room" in the main hall of Warsaw University of Technology	Z+F 5006	360°	320°	6.3 mm/10 m	8	28,722,210
VI - "Empty Shopping Mall"	Z+F 5006	360°	320°	12.1 mm/10 m	7	13,677,292

3 Methodology

3.1 Test Sites description

This investigation aimed to analyse the application of "standard" and affine detectors for automatic non-signalised tie point detection in automatic TLS data registration. The selection of the detector was performed in six different locations: historical 17th-century basements of the Royal Castle in Warsaw, Poland, without the decorative structure (Test Site I and II), Museum of King Jan III's Palace at Wilanów, Warsaw, Poland, with decorative elements, ornaments, and materials on walls (Test Site III) and flat frescos (Test Site IV), a narrow office (Test Site V) located in the main hall of Warsaw University of Technology, and a shopping mall "Serenada" located in Krakow, Poland (Test Site VI) (Figure 3). TLS data were acquired with the use of two phase-shift scanning instruments: the Z+F 5003 and Z+F 5006h. Table 1 describes TLS point clouds used in this investigation.

The selection of these Test Sites was motivated by their varied characteristics, the number of ornaments and architectural details, as well as their characteristic texture, which significantly affects the effectiveness of key points detection using hand-crafted detectors:

- Test Sites I and II (Figure 3a) include brick-and-mortar structures with irregular shapes, featuring arch-shaped ceilings ranging from approximately 2.1 m to 3.2 m in height. Owing to historical attributes and prevailing humidity, sections of the rooms exhibit damp walls and crumbling brick fragments, making the placement of designated control points impractical. In addition, the placement of the tripod is not possible due to room size constraints. Implementing a target-based methodology would require multiple locations of the scanner, resulting in inaccurate point cloud registration. The basement was divided into Test Sites I and II, a regularly shaped facility (approx. 5.6 m × 5.1m) however, a centrally located ventilation pipe limited the flexibility of the scanner station placement. Test Site II (7.4 m × 5.1 m) with curves at 1/3 and 2/3 distances, recesses, and long window panes, required additional signal points and scanner positions.
- Test Site III, "The Queen's Bedroom," (Figure 3b), is characterised by geometric complexity, including rich ornaments, bas-reliefs, facets, mirrors in golden frames, decorative fireplaces, and wall-hanging fabrics. The site is approximately 6.4 m × 7.3 m × 5.3 m.
- Test Site IV, "The Chamber with a Parrot," (Figure 3c), features minimal ornaments and lacks bas-reliefs, facets, or fabrics. Instead, the walls feature painted patterns imitating spatial effects. The dimensions of "The Chamber with a Parrot" are approximately 4.2 m × 4.2 m × 2.6 m.
- Test Site V (Figure 3d) is used as an office with smooth-textured walls, ceiling-mounted lamps and power wires, and a dark-carpeted floor. The dimensions of the office room are approximately 7.4 m × 5.9 m × 4.5 m.
- Test Site VI, the "Empty Shopping Mall" (Figure 3e), features smooth-textured walls, a concrete floor, ceiling-mounted lamps, electric wires, and an air-conditioning system. The dimensions of the empty shopping mall are approximately 21.5 m × 7.1 m × 6.3 m.

3.2 Overview of the Approach

This study aims to assess the improvement in quality and completeness of the TLS registration process affine detector the results obtained using selected detectors and affine detectors (blob and corner) in the multi-stage TLS registration process were compared, which involved the following steps: (1) The software was developed to automatically convert 3D point cloud data into the form of a 2D spherical representation with a depth map; (2) commonly-used corner detectors (FAST, BRISK) and blob detectors (CenSurE, SURF and SIFT) were tested; (3) Authors implemented the affine detectors: AFAST, ABRISK, ACenSurE, ASURF based on the ASIFT approach; (4) Structure-from-Motion (SfM) was used to determine the tie points to perform the pairwise TLS registration; (5) the geometrical quality of tie points was verified using covariance analysis. Figure 4 presents the proposed methodology. The influence of detector selection on the accuracy, completeness and orientation time of point clouds will be analysed in this article as a crucial element affecting the final accuracy of TLS point cloud registration.

To evaluate the suitability of the detectors mentioned above, rasters at full resolution (based on raw data point clouds) were generated, making the interpolation of coordinate values for pixels unnecessary. Because the data were acquired using a fixed scanning interval, it was possible (using the scanner's SDK – Software Development Kit) to use the vertical and horizontal angle values and the measured distance to generate spherical images. The incorporated raster grey level values were acquired from the intensity of the laser beam reflection recorded by the Z+F 5006h and Z+F 5003 scanners. Additionally, the total station measurements were performed for Test Sites I and II, and data were adjusted with the $RMSE_X$ = 2.2 mm, $RMSE_Y$ = 1.3 mm, and $RMSE_Z$ = 0.4 mm. Those points were used for an independent quality analysis pertaining to Test Sites I and II (Markiewicz et al., 2021).

The proposed approach to point cloud orientation using SfM consists of the following steps:

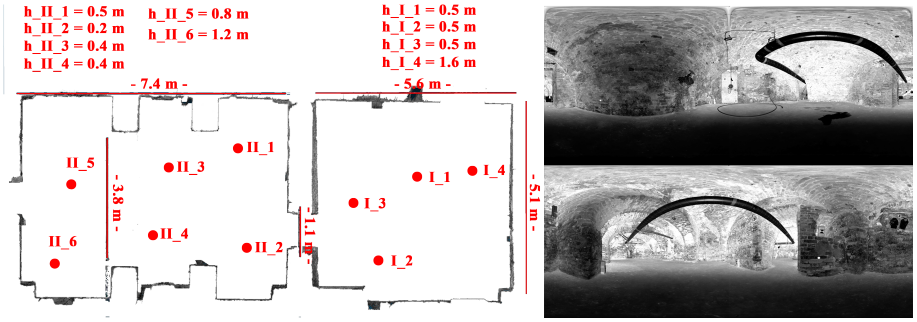

(a)

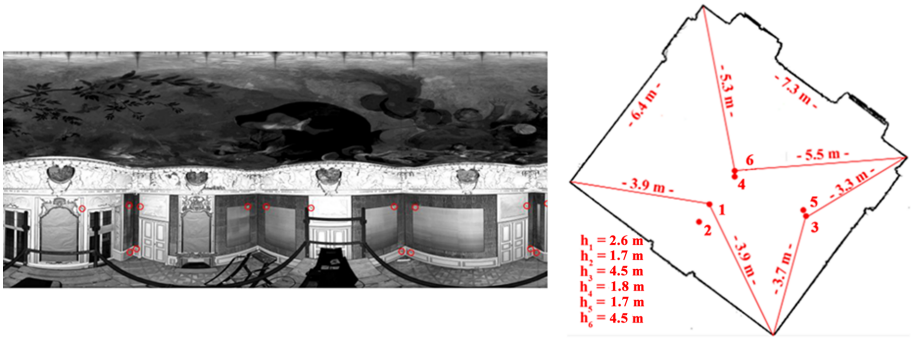

(b)

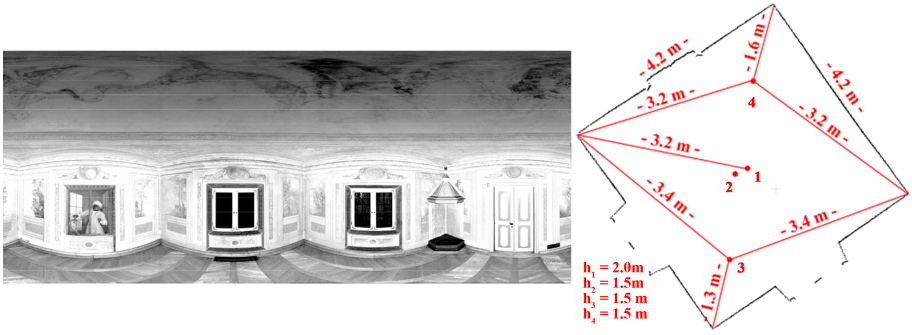

(c)

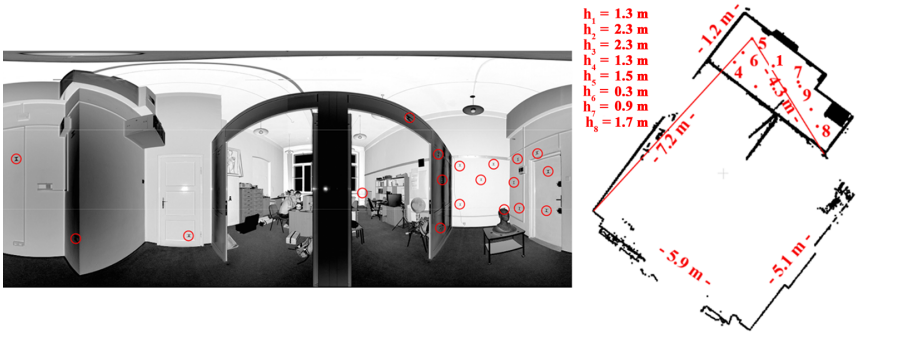

(d)

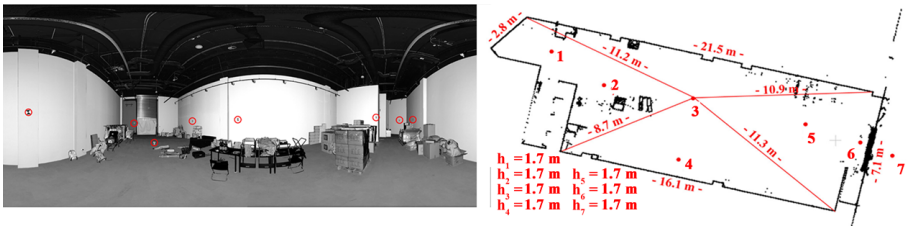

(e)

Figure 3. The floor plan with marked dimensions and TLS positions (red dots). Spherical representation with marked reference points (red circles). For each TLS position, the height (h) is presented. (a) Test Sites I and II: Basement in the Royal Castle (Markiewicz et al., 2023); (b) Test Site III: "The Queen's Bedroom" (Markiewicz et al., 2023); (c) Test Site IV: "The Chamber with a Parrot" without marked points (Markiewicz et al., 2023); (d) Test Site V: "The office room" (Markiewicz et al., 2023) and (e) Test Site VI: "The empty shopping mall" (Markiewicz et al., 2023)

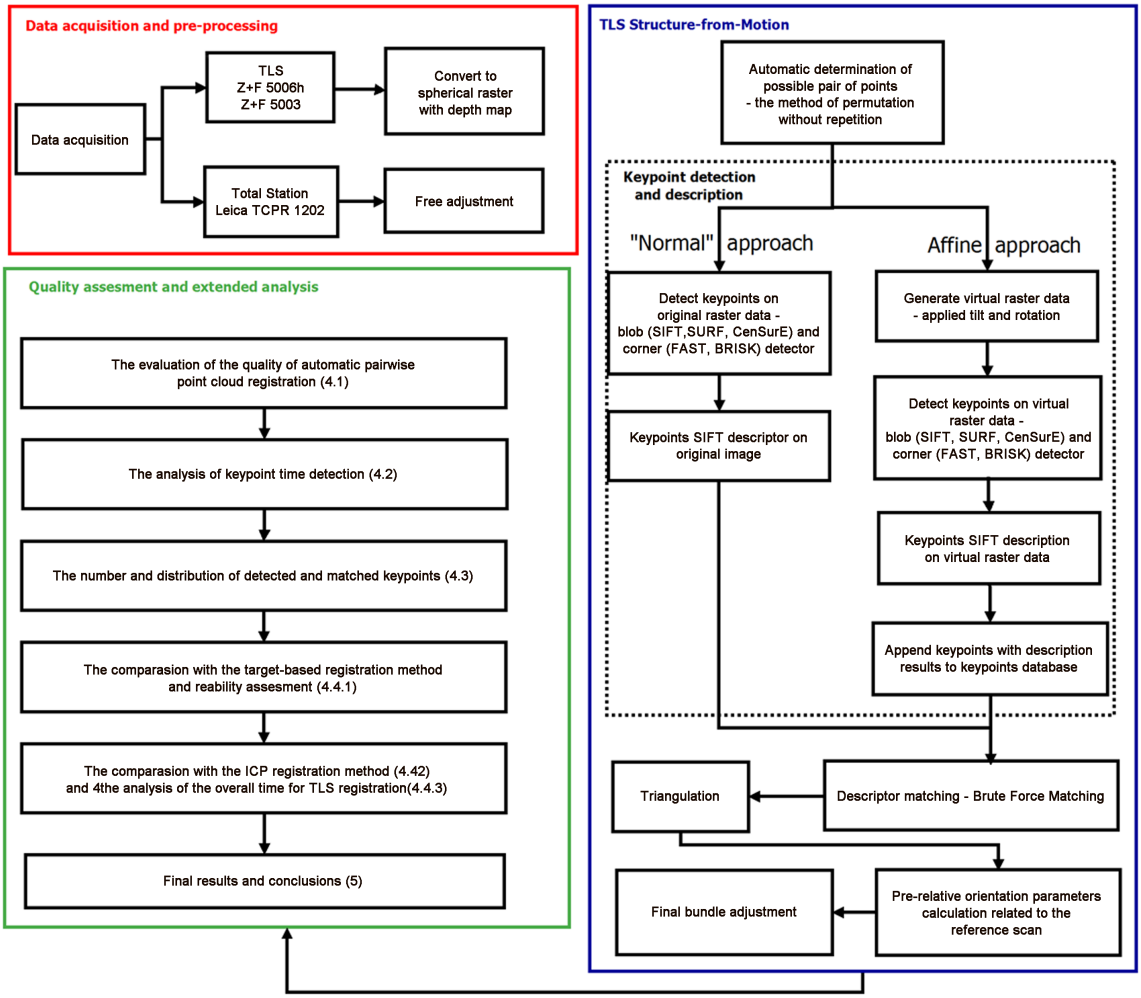

Figure 4. Diagram of the proposed methodology of TLS data registration

i. determination of the pair of rasters using the methods of permutations without repetitions:

$$\binom{n}{k} = \frac{n!}{k!\,(n-k)!} \tag{4}$$

where $k = 2$ (a pair of scans), n is the number of all scans;

ii. detection of key points with affine detectors;

iii. description of all detected key points by SIFT descriptor;

iv. descriptor matching with the use of Brute Force matching;

v. geometrical verification of the detected tie point, performed in the iterative process (RANSAC method) with the following assumptions: full registration (the accuracy on control and check points not exceeding 5mm and covariances factors higher than 0.5), initial registration used for final registration bases on the ICP (threshold 10 mm) and non-registration (values on control and check higher than 10 mm);

vi. final bundle adjustment of scans.

The following factors were analysed to assess the quality and completeness of the TLS registration process:

- the completeness of data registration that determined the robustness of the proposed method and the effectiveness of the proposed solution,
- the time of key point detection,
- the number of key points detected,
- the registration accuracy on natural and marked check points with reliability assessment,
- the distance between pairs of point clouds for the proposed method and state-of-the-art approaches: Iterative Closest Point and Target-based,
- the overall time of point cloud registration with the feature-based method and state-of-the-art approaches.

4 Results and Discussion

4.1 The evaluation of the quality of automatic pairwise point cloud registration

To assess the detectors' or affine detectors' applicability in the TLS registration process, all possible pairs of overlapping point clouds acquired from different heights and distances from the scanned surfaces were considered. The results of this investigation are presented in Figure 5. To interpret the results, the registration results were colour-coded according to the methodology presented in Markiewicz et al. (2023): (1) green – the complete registration with the $RMSE_X$, $RMSE_Y$ and $RMSE_Z \leq 0.005$ m and covariance factor > 0.5; (2) orange – preliminary registration obtained parameters should be treated as the initial parameters for Iterative Closest Point (ICP) registration and (3) red – no registration because the points were not well distributed an d/or the RMSE < 0.01 m and/or covariance < 0.5. Additionally, due to the processing of point clouds of wall fragments (rather than the entire room) on Test Site III, it was decided to mark "x" pairs of scans that do not overlap.

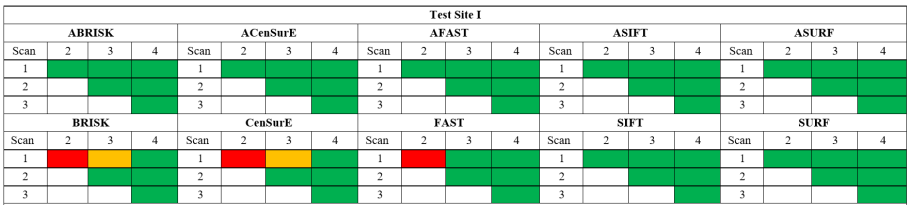

(a)

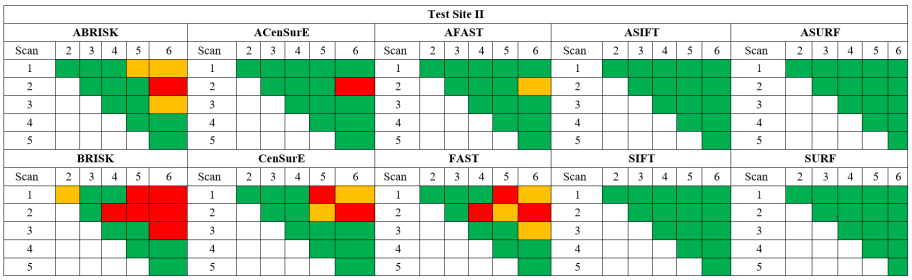

(b)

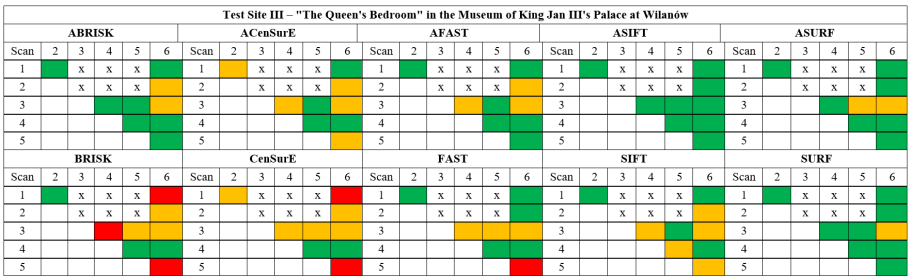

(c)

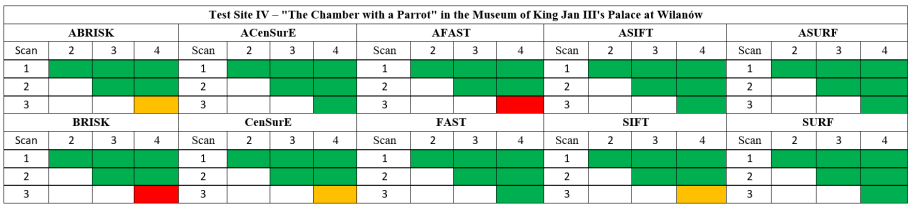

(d)

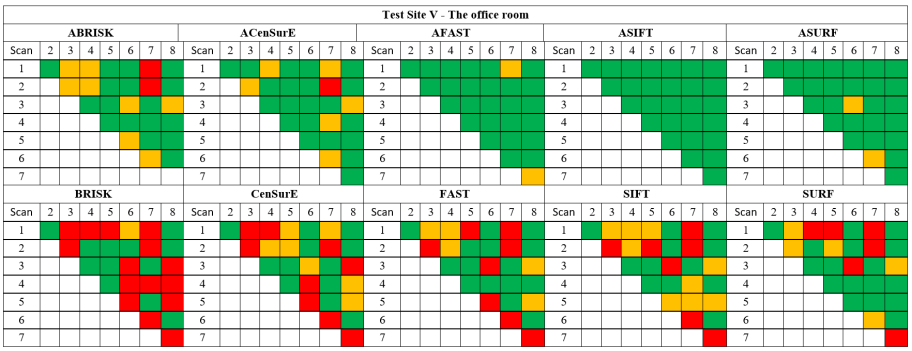

(e)

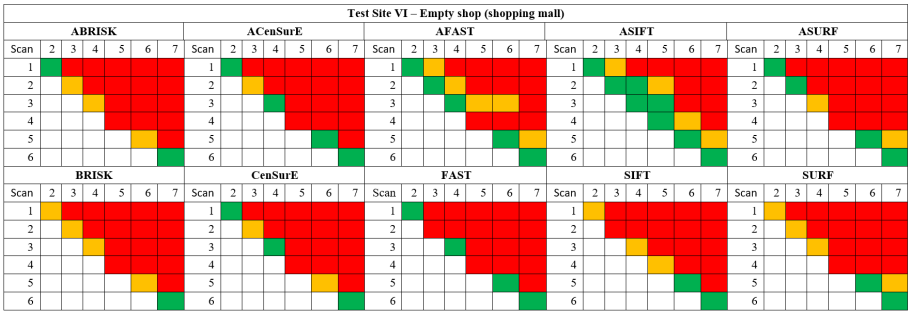

(f)

Figure 5. The accuracy of the TLS registration for detectors and affine detectors: (a) and (b) Test Sites I and II: Basement in the Royal Castle; (c) Test Site III: "The Queen's Bedroom"; (d) Test Site IV: "The Chamber with a Parrot"; (e) Test Site V: "The office room" and (f) Test Site VI: "The empty shopping mall"

The assessment of the correctness and completeness of the matching pair of scans for all test sites (Figure 5) was only possible using the AFAST (point detector) and ASIFT (blob detector), so the remaining algorithms should be evaluated separately for each test field.

- The lowest number of correct matched pairs of scans was obtained for the BRISK detector. For Test Site I – only 4 of 6, Test Site II – 8 of 15, Test Site III – 3 of 9, Test Site IV – 5 of 6, Test Site V – 12 of 28, and Test Site VI – 1 of 21 pairs of scans was correctly registered (full orientation).
- For CenSurE detector, there is a slight improvement as compared to the results for BRISK. Using this detector, it was possible to register correctly for Test Site I – 4 of 6, Test Site II – 11 of 15, Test Site III – 2 of 9, Test Site IV – 5 of 6, Test Site V – 12 of 28, and Test Site VI, 3 of 21 pairs of scans.
- FAST (corner detector) enabled all pairs of scans register for Test Site IV only. For the other pairs of point clouds, the higher number of corrected matched pairs of scans were obtained than for BRISK and CenSurE, and it was possible to register only for 5 of 6 pairs of scans for Test Site I, 9 of 15 for Test II, 5 of 9 for Test Site III, 15 of 28 for Test Site V, and 4 of 21 for Test Site III.
- The full registration was successful for Test Sites I and II for the blob SIFT detector. For other test sites, 4 of 9 for Test Site III, 5 of 6 for Test Site IV, 11 of 28 for Test Site V, and 2 of 21 for Test Site VI were registered correctly.
- For the blob SURF detector, registering all pairs of scans was possible for Test Sites I, II and IV. For other cases, 8 of 9 for Test Site III, 17 of 28 for Test Site V, and 2 of 21 for Test Site VI pairs of scans were correctly registered.

The correctly determination of the TLS pair of point clouds registration is crucial for multi-position TLS registration. This clearly affects the possibility of global registration of all possible point clouds and results in the robustness and accuracy of the entire process. In summary, the results shown in Figure 5 clearly indicate that it was possible to carry out multi-position TLS registration for Test Site I with all detectors except the BRISK, CenSurE and FAST detectors, Test Site II, III and V for all detectors, and Test Site IV excepted BRISK. The use of "standard" detectors did not allow for a full registration of all scans, only selected pairs for Test Site VI.

A potential solution to a full registration could be the use of affine detectors for tie point extraction. In this study, for Test Site I, only ACenSurE was capable of a pairwise registration with only one pair of scans (with the CenSurE detector, two pairs of scans were not correctly registered). For Test Site II–V, using affine detectors enabled global TLS registration using all algorithms. As in the case of the results obtained by the "standard" detectors, the lowest number of correctly matched pair of point clouds were obtained for Test Site VI, but a full registration using the ASIFT and AFAST detectors was possible.

Summarising the results of the correctness and completeness of point cloud registration using "standard" and affine detectors, it can be stated that:

- The least successful point clouds registration results were obtained for the BRISK detector. The biggest problems occurred for pairs of point clouds for which the corresponding parts were measured at significantly different angles to the normal surface of the vector (i.e., acute angles to the normal surface of the vector) and for significantly different distances from the scanner position. This contributed to various 'distortions' in the rasters resulting from converting point clouds from the 3D to the 2D form. In the BRISK detector, neighbouring pixels within a circle of 16 pixels (a Bresenham circle of radius 3) on different scale-spaces are used to assess whether a potential pixel should be treated as a corner or not. For this reason, the "change of scale" mapping in the compared spherical images of corresponding fragments affects the inability to detect potential tie points. In addition, the correctness and completeness of the TLS point cloud pairs registration are affected by the accuracy of key point determination, which is dependent on the accuracy of the TLS measurement.
- The operation of the BRISK detector is based on the same assumptions regarding the comparison of neighbouring pixels within a circle of 16 pixels as implemented in the FAST detector, but in contrast to the FAST detector, it considers an additional evaluation based on scale-space searching. Therefore, the influence of surface scanning angles and the distance between the scanner position and the object to be imaged is the same as that of the BRISK detector. Still, a full-resolution search of the spherical image (without scale-space verification) allows for the detection of more key points compared to BRISK, which in further stages are used to pair TLS point cloud registration. For this reason, a larger number of correctly registered scan pairs is possible to obtain with the FAST algorithm.
- The SIFT, SURF and CenSurE algorithms are blob detectors and, in contrast to point detectors (BRISK and FAST), are based on the greyscale gradients and are, therefore, scale-invariant and more robust. The results differ due to the filters and methods used in feature point detection. In addition, the CenSurE algorithm searches for extremes at full image resolution while the SIFT and SURF detectors detect points at different pyramid levels. This made it possible to detect more tie points than the number of points detected using point detectors, translating into an increase in the number of correctly registered pairs of scans. Despite this, as with the FAST and BRISK detectors, they do not allow for the correct registration of point clouds, for which overlapping fragments are characterised by a significant "distortion" on spherical images (Test Site V and VI). The lowest number of correct matched pairs of scans for the three blob detectors was obtained for CenSurE, which is caused by detecting key points on the full-resolution image and on the spherical image for which the grey levels were generated from the raw intensity.
- In summary, the solution to the problems of correct matching of point cloud pairs (regardless of significantly different angles to the standard surface of the vector different distances from the scanner position) lies in the use of affine detectors. It has significantly improved TLS point cloud pairwise and multi-stage registration, and the use of ASIFT and AFAST has enabled the minimum point cloud pairwise registration necessary for final multi-position registration for all test sites.

4.2 The analysis of key point time detection

To evaluate the detection time of the feature points, individual detectors and affine detectors were employed as a single-thread solution. The key point search process was repeated 50 times, making it possible to compute the average detection time for a single key point. Figure 6 shows the average detection time for a single key point.

Each detector can detect different numbers of points on the same point clouds converted to the raster format. Therefore, the detection time of a single feature was calculated. The values shown in Figure 6 indicate that the shortest key points detection time was obtained by the FAST point detector (average for all Test Sites was 0.001 ms) and the longest for the CenSurE blob detector (average for all Test Sites – 0.524 ms). For the other "standard" detectors, key points search times were the

Table 2. The average number of detected key points and ratio between detected key points by affine and "standard" detector

Detector	Number of Keypoints			Ratio between detectors			Number of Keypoints			Ratio between detectors		
	Test Site I	Test Site II	Test Site III	Test Site I	Test Site II	Test Site III	Test Site IV	Test Site V	Test Site VI	Test Site IV	Test Site V	Test Site VI
BRISK ABRISK	14686 120866	12415 97533	2562 22210	8.2	7.9	8.8	1308 18110	2664 33725	4842 50108	10.5	15.4	10.1
CenSurE ACenSurE	6504 78132	4928 51666	1395 13244	12	10.5	9.5	857 20372	1712 33195	3057 45341	23.6	20.7	14.8
FAST AFAST	259589 2425131	227549 2179661	37746 369125	9.3	9.6	9.8	85474 503587	29192 350084	44950 438960	5.9	12.1	9.8
SIFT ASIFT	75426 932974	68967 856564	10776 152601	12.4	12.4	14.3	18672 223525	10089 162695	12662 190659	12	16.2	15
SURF ASURF	106442 1463700	103118 1401474	21554 260185	13.8	13.6	12.4	71235 895272	34517 557614	38336 542328	12.4	16.2	14.1

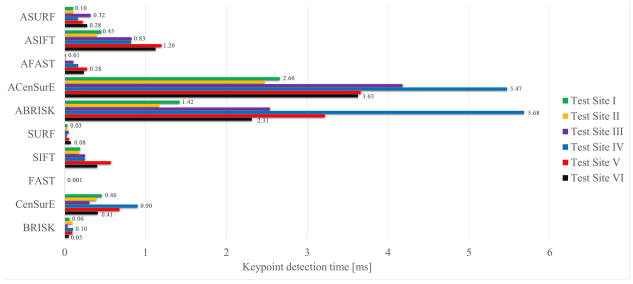

Figure 6. The consumption of each detector

longest for SIFT, BRISK and SURF, respectively.

A comparison of the point detection time results based on "standard" detectors and affine detectors shows that the time is, on average, longer for detecting key points using point detectors rather than blob detectors. The most significant difference was obtained for the AFAST algorithm – almost 312 times longer. However, considering the time in milliseconds, it is still shorter than for the BRISK, CenSurE, or SIFT detectors. In the case of the BRISK detector, the difference is about 46 times higher, and the values are between 12 and 56. Comparing the differences in point detection time by blob and point a-detectors, the processing time is significantly shorter, averaging 9 times for the CenSurE detector, 3 times for the SIFT and 4 times for the SURF "standard" detector. The smallest deviations in the ratio (affine detector to detector) were observed for the ASIFT and ASURF detectors, and the single key points search time for the ASURF detector was shorter than for the CenSurE and SIFT detectors.

4.3 The analysis of the number and distribution of detected and matched key points

To evaluate the influence of the affine detector in the TLS registration process and selection of point detectors (FAST, BRISK, AFAST and ABRISK) and blob (SIFT, SURF, CenSure, ASIFT, ASURF and ACensure), the detected key points were analysed. Table 2 presents the average number of key points and the ratio between points detected by the affine and the "standard" detector.

The average number of detected key points presented in Table 2 indicated that the most significant number of key points was obtained by FAST, SURF, SIFT, BRISK and CenSurE detectors for all test sites. The ratio between the best (FAST) and worst (CenSurE) results for Test Site I is about 40, for Test Site II is 46, for Test Site III is 27, for Test Site IV is 100, for Test Site V is 17, and for Test Site VI is 15. However, when the number of key points detected by SIFT and SURF are compared with the FAST detector, the ratio is about 3.5 for the SIFT detector and 1.6 for the SURF detector measured for all test sites.

The results presented in Table 2 also show that using affine detectors allowed the detection of a significantly larger number of key points than with "standard" detectors. For the point detectors (ABRISK and AFAST), the number of detected key points increased by 8–12 times and for blob detectors (ACenSurE, ASURF and ASIFT) by about 10–24 times.

The spatial distribution of tie points should also be considered to verify which detector is more appropriate for correct TLS point cloud registration,affecting the registration quality and final process accuracy. In Figures 7–12, the tie points distribution was shown for cases for which full bundle adjustment was possible and for which only part of the scans could be registered (marked with a cross in the description).

The results presented in Figures 7–12 indicate that, generally, with the affine detectors, as compared to the "standard" detectors, it is possible to find more correct distributed tie points in terms of reliability theory that guarantee a correct point cloud registration. The obtained results should be assessed independently for each Test Site:

- **Test Site I and II**: The distribution of tie points for all methods (detectors and affine detectors) is similar for Test Site I. For standard and affine algorithms, the most points (highest density) were detected and used on the two walls visible on all scans. Significantly fewer points are on the ceiling, and the highest density was obtained in the central part of the basement for SIFT/ASIFT, SURF/ASURF and AFAST. For the BRISK/ABRISK and CenSurE/ACenSurE methods, fewer points were detected (compared to the algorithms discussed above), and most of them were distributed on the walls mapped on all scans and a small number on the ceiling. However, it should be emphasised that the number and distribution of points allowed for the correct registration of all point clouds.
- **Test Site III**: For Test Site III, containing rich ornaments, bas-reliefs, and facets, the distribution of tie points was better for affine detectors than the "standard" case because the density of points was higher, and the points were evenly distributed over the whole area. Considering only the case of "standard" detectors, the results (distribution and number of points) were obtained for the respective SURF, FAST and SIFT approaches.

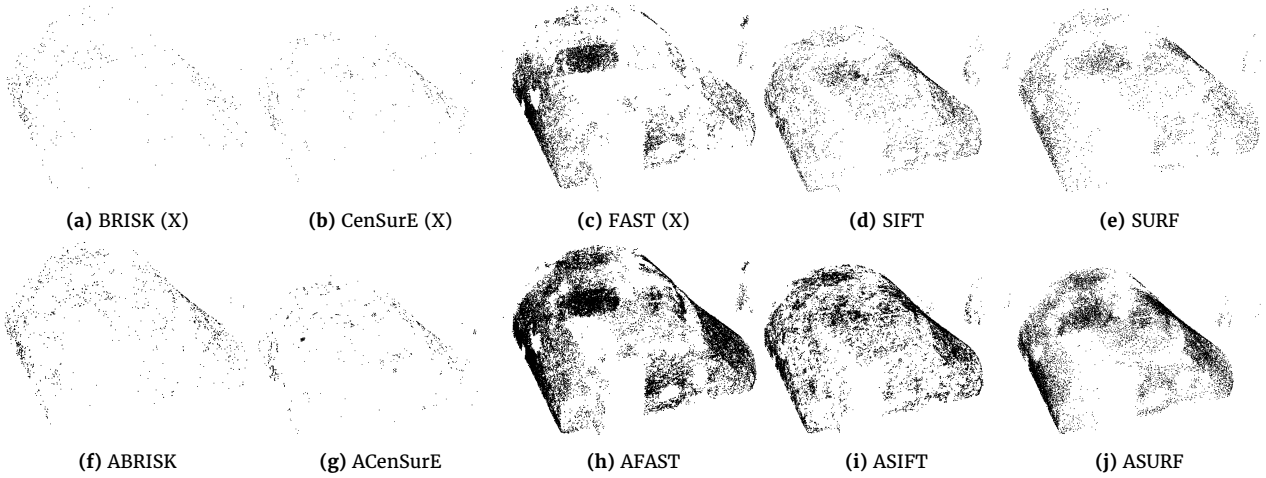

(a) BRISK (X) **(b)** CenSurE (X) **(c)** FAST (X) **(d)** SIFT **(e)** SURF

(f) ABRISK **(g)** ACenSurE **(h)** AFAST **(i)** ASIFT **(j)** ASURF

Figure 7. The distribution of tie points used for TLS point cloud registration for each method – Test Site I. Marked with X cases for which full bundle adjustment was impossible.

- **Test Site IV** as in the previous Test Sites, more points were detected, and a evenly distribution was obtained using affine detectors than in the "standard" case. There is a noticeable uneven point density throughout the study area, which follows from the way the algorithms work. Higher point densities are noticeable for areas with significant changes in grey degree gradients. However, crucially, this should not be seen as a problem, as detecting a considerable number of points allows for additional (but not obligatory) data filtering to obtain an even distribution of points. As in the case of previous Test Sites, the BRISK, CenSurE (and their affine equivalents) detectors allowed a sufficient number of correctly positioned binding points to be detected based on which full point cloud registration could be performed.
- **Test Site V**: The highest density, most similar numbers, and tie point density results were obtained for the office (public facility) for AFAST, ASIFT, ASURF, FAST, and SURF algorithms. Like Test Site IV, the lowest number of points were obtained for the BRISK and CenSurE approaches despite point clouds being registered. This is due to the characteristics of the test site, including the absence of significant changes in gradients (plain wall) and being equipped with furniture and office devices (affecting the quality of the point cloud, e.g., through erroneous edge delineation due to mixed-edge effects).
- **Test Site VI**: Similar to the analysis of the correctness of the pairwise point cloud matching, only the distribution of binding points detected with the ASIFT and AFAST detectors allowed for a full point cloud registration, due to the generation of 2D intensity rasters converted from 3D point clouds and the existence of distortion and wide-based point clouds. Therefore, when planning a survey of facilities, i.e., shops in shopping centres, deciding whether to use ASIFT or AFAST detector or set up additional scanner positions to reduce the baseline between point clouds and utilise any affine detector algorithms is crucial.

4.4 A comparison of feature-based TLS registraon with commonly used methods

In order to verify the accuracy of point cloud orientation using affine detectors and intensity rasters, it is necessary to compare the results with those obtained using other point cloud registration methods. Two commonly-used point-based methods: target-based implemented in Z+F LaserControl software (Z+F, 2024) and ICP implemented in the open-source CloudCompare (Cloudcompare, 2024) were used in this study. In addition, the overall time for TLS point cloud registration was compared based on different data processing methods.

The target-based method

The target-based method is one of the most commonly used methods of TLS point clouds registration. It is usually based on signalised points detected semi-automatically or automatically and, less often, manually. For this reason, it is widely used and implemented in many commercial applications. Therefore, a comparison was made between the results obtained using "standard" and affine detectors with those from the Z+F LaserControl software dedicated to Z+F scanners (used in this study). Additionally, the covariance ratio values were compared to assess the point distribution automatically (in accordance with reliability theory). Table 3 presents the results of the investigation.

An evaluation of the results shown in Table 3 shows that the differences in RMSE at the signalled check points (obtained from multi-position TLS registration) are different for Test Sites and are between -3.9 mm and 3.4 mm. A slight improvement for a-detectors in the data orientation process for ASIFT (0.5 mm) and ASURF (1.8 mm) occurs for Test Site I. For ABRISK, ACenSurE and AFAST, the maximum differences in RMSE values are higher than -1.0 mm for the X-coordinate, 3.9 mm for the Z-coordinate and 0.5mm for the X-coordinate, respectively. In the case of Test Site II, a slight decrease in accuracy for all affine detectors is expected for ASIFT (0.9 mm for X-coordinate). It does not exceed 0.8 mm for ABRISK, ACenSurE, and AFAST algorithms and 2.2 mm for ASURF. For Test Site III, a significant drop is seen for ACenSurE (on average, 3.0 mm for all coordinates), ABRISK (on average, 2.1 mm for all coordinates), ASURF (on average, 0.6 mm for all coordinates) and AFAST (on average, 0.1mm for all coordinates). Yet, there is an improvement for ASIFT with 0.5 mm on average. For Test Site IV, using affine detectors in the data orientation process slightly decreased the RMSE values for all coordinates for all detectors and did not exceed 0.8 mm.

According to the internal reliability theory, the values of indicators are in between <0,1>, and (1) if the value is equal to 0, the point is completely uncontrolled; (2) if the value is equal to 1, the point is fully controllable by other points and (3) if the value is ≥ 0.5, this contributed to fulfilling the network's controllability condition (Markiewicz et al., 2021). The significant

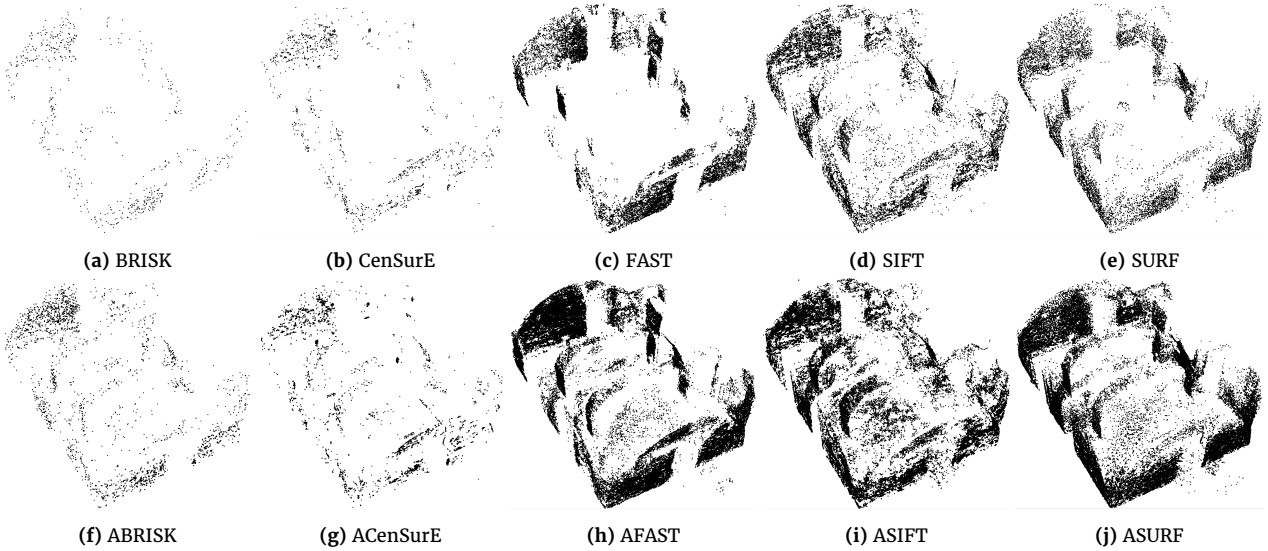

(a) BRISK **(b)** CenSurE **(c)** FAST **(d)** SIFT **(e)** SURF

(f) ABRISK **(g)** ACenSurE **(h)** AFAST **(i)** ASIFT **(j)** ASURF

Figure 8. The distribution of tie points used for TLS point cloud registration for each method – Test Site II.

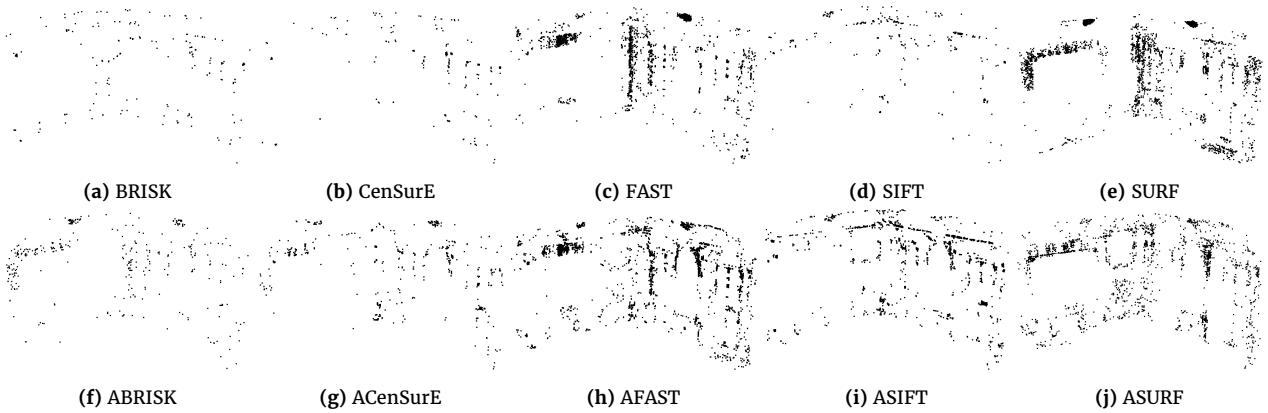

(a) BRISK **(b)** CenSurE **(c)** FAST **(d)** SIFT **(e)** SURF

(f) ABRISK **(g)** ACenSurE **(h)** AFAST **(i)** ASIFT **(j)** ASURF

Figure 9. The distribution of tie points used for TLS point cloud registration for each method – Test Site III.

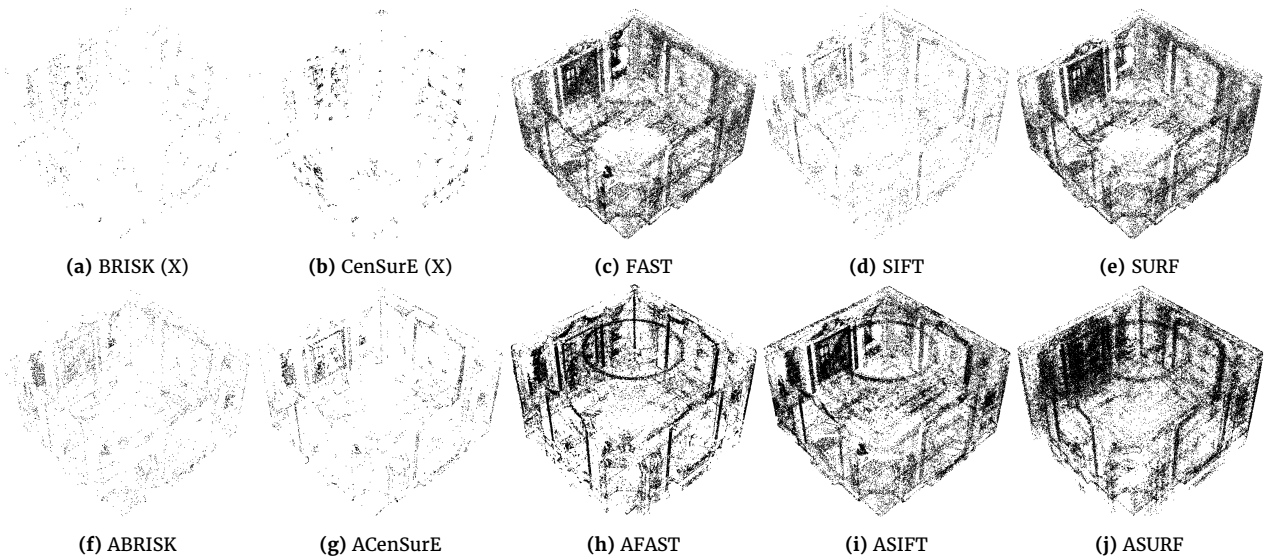

(a) BRISK (X) **(b)** CenSurE (X) **(c)** FAST **(d)** SIFT **(e)** SURF

(f) ABRISK **(g)** ACenSurE **(h)** AFAST **(i)** ASIFT **(j)** ASURF

Figure 10. The distribution of tie points used for TLS point cloud registration for each method – Test Site IV. Marked with X cases for which full bundle adjustment was impossible.

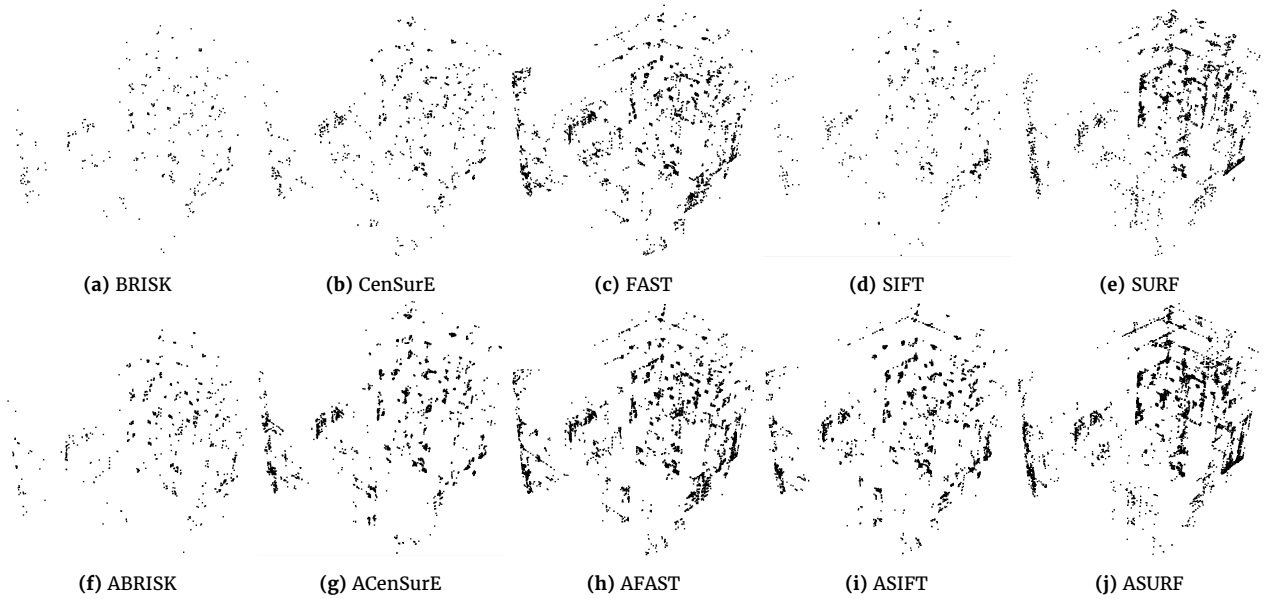

(a) BRISK **(b)** CenSurE **(c)** FAST **(d)** SIFT **(e)** SURF

(f) ABRISK **(g)** ACenSurE **(h)** AFAST **(i)** ASIFT **(j)** ASURF

Figure 11. The distribution of tie points used for TLS point cloud registration for each method – Test Site V.

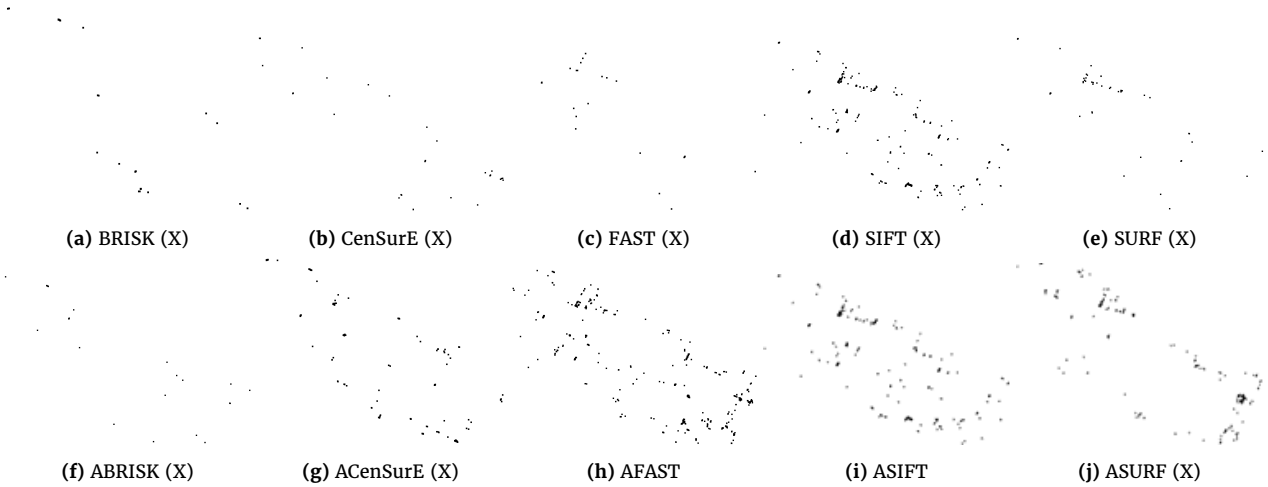

(a) BRISK (X) **(b)** CenSurE (X) **(c)** FAST (X) **(d)** SIFT (X) **(e)** SURF (X)

(f) ABRISK (X) **(g)** ACenSurE (X) **(h)** AFAST **(i)** ASIFT **(j)** ASURF (X)

Figure 12. The distribution of tie points used for TLS point cloud registration for each method – Test Site VI. Marked with X cases for which full bundle adjustment was impossible.

Table 3. Comparison of results of TLS full registration method for all scans and the target-based registration method with reliability assessment for all Test Sites

Detector	RMSE on Marked Check Points [mm] Test Site I			The Reliability indices Test Site I			RMSE on Marked Check Points [mm] Test Site II			The Reliability indices Test Site II			RMSE on Marked Check Points [mm] Test Site III			The Reliability indices Test Site III		
	X	Y	Z	Min	Avg	Max	X	Y	Z	Min	Avg	Max	X	Y	Z	Min	Avg	Max
BRISK	5.80	5.70	5.70	0.11	0.91	0.98	5.10	5.40	5.10	0.15	0.90	0.98	2.20	2.50	2.20	0.04	0.80	0.96
ABRISK	4.80	4.80	5.20	0.33	0.98	0.99	5.70	5.70	5.70	0.88	0.98	0.99	4.30	4.90	4.10	0.14	0.89	0.98
CenSure	3.60	5.70	6.40	0.02	0.92	0.97	2.60	2.50	2.40	0.13	0.96	0.99	3.40	3.20	3.10	0.08	0.88	0.98
ACenSure	3.00	2.70	2.50	0.00	0.98	0.99	3.30	3.30	3.20	0.89	0.99	1.00	5.90	7.20	5.60	0.04	0.89	0.97
FAST	3.90	3.70	3.70	0.92	0.99	1.00	3.40	3.30	3.40	0.65	0.99	1.00	2.20	2.20	2.20	0.10	0.99	1.00
AFAST	3.40	3.40	3.40	0.94	0.99	1.00	4.00	3.60	4.00	0.97	0.99	1.00	2.30	2.20	2.30	0.15	0.98	0.99
SIFT	1.40	1.30	1.30	0.92	0.99	1.00	2.30	2.30	2.30	0.65	0.99	1.00	2.40	2.30	2.40	0.01	0.86	0.98
ASIFT	1.80	1.80	1.80	0.98	0.99	1.00	1.40	1.50	1.50	0.95	0.99	1.00	1.90	1.90	1.80	0.40	0.96	0.99
SURF	2.00	2.00	2.00	0.82	0.98	0.99	2.70	2.70	2.80	0.92	0.99	1.00	3.21	3.22	4.12	0.35	0.99	1.00
ASURF	3.70	3.70	3.80	0.96	0.99	1.00	4.90	4.90	5.00	0.98	0.99	1.00	4.20	4.00	4.10	0.20	0.98	0.99
Target-Based Method	2.50	2.00	1.40	0.35	0.67	0.85	2.50	2.40	2.80	0.01	0.20	0.62	3.30	3.50	2.60	0.22	0.41	0.68

Detector	RMSE on Marked Check Points [mm] Test Site IV			The Reliability indices Test Site IV			RMSE on Marked Check Points [mm] Test Site V			The Reliability indices Test Site V			RMSE on Marked Check Points [mm] Test Site VI			The Reliability indices Test Site VI		
	X	Y	Z	Min	Avg	Max	X	Y	Z	Min	Avg	Max	X	Y	Z	Min	Avg	Max
BRISK	2.1	2.2	2.2	0.08	0.98	0.99	4.8	5.2	4.5	0.05	0.83	0.98	x	x	x	x	x	x
ABRISK	2.1	2.3	2.2	0.57	0.97	0.99	2.4	2.8	2.5	0.63	0.95	0.99	x	x	x	x	x	x
CenSure	1.4	1.4	1.3	0.7	0.99	1	5.8	5.4	5.2	0.51	0.94	0.99	x	x	x	x	x	x
ACenSure	2.1	2.1	2.1	0.8	0.99	1	2.2	2.2	2.1	0.87	0.98	0.99	x	x	x	x	x	x
FAST	1.7	1.8	1.8	0.89	0.99	1	5.7	5.6	5.6	0.67	0.98	0.99	x	x	x	x	x	x
AFAST	1.8	1.9	1.9	0.99	0.99	1	2	2	2	0.92	0.99	1	9.0	9.2	9.0	0.01	0.91	0.98
SIFT	1.2	1.3	1.3	0.86	0.99	1	3.8	3.9	3.5	0.11	0.92	0.98	x	x	x	x	x	x
ASIFT	1.6	1.6	1.6	0.99	1	1	1.8	1.8	1.8	0.92	0.99	1	4.7	4.6	5	0.03	0.94	0.98
SURF	1.7	1.8	1.8	0.95	0.99	1	5.2	5.3	5.4	0.77	0.97	0.99	x	x	x	x	x	x
ASURF	1.8	1.8	1.8	0.99	1	1	2.1	2	2	0.93	0.99	1	x	x	x	x	x	x
Target-Based Method	1.8	1.4	1.6	0.23	0.46	0.71	2.2	2.4	1.7	0.29	0.72	0.95	4.2	3.7	3.6	0.28	0.7	0.99

x – insufficient number of tie points

impact of using affine detectors is evident from the minimum, maximum and mean covariance factors. This improves the geometric distribution of tie points for the minimum values (an increase from 0.05 to 0.63 – to a value above 0.5, which is the threshold value). In the case of Test Site I, using the affine BRISK and CenSurE detector did not affect the increase of the minimum value of the covariance factor, nor for Test Site II detectors. It should also be noted that the use of affine detectors has a significant effect on the pattern of mean and maximum covariance factors.

The results in Table 3 show that the registration process accuracy at the signalled check points is close to the commonly used target-based approach. For Test Site I, the average differences between RMSE values for all coordinates ranged from -0.2 mm to 1.8 mm for all a-detectors expected ABRISK (the average value is 3.0 mm). For other detectors, the average differences were in the range of -0.6 mm to 1.8 mm for FAST, SIFT and SURF algorithms, 3.3 mm for CenSurE and 3.8 mm for BRISK. Considering the covariance factors, using the detector-based method significantly increases the controllability of the network. For the detector-based method, the average is between 0.91–0.99, while for the target-based method, the average is 0.67.

In the case of Test Site II, both the detector and affine detector results are comparable. Hence, deciding if using affine detector is necessary is not straightforward. It should be noted that the average RMSE values obtained for the detectors and the target-based method are comparable. In the case of the detectors, the differences were 2.6 mm, -0.1 mm, 0.8 mm, -0.3 mm, and 0.2 mm for BRISK, CenSurE, FAST, SIFT and SURF, respectively. The difference between mean RMSE values from affine detectors and the target-based method are: ABRISK 3.1 mm, ACenSurE 0.7 mm, AFAST 1.3 mm, ASIFT -1.1 mm, and ASURF 2.4 mm. The average covariance factor values (0.95) are about 4.5 times lower than the target-based method (0.2).

For Test Site III, the RMSE's values on points detected by BRISK and FAST were similar on detectors (approximately 1.2 mm) to BRISK, FAST, and SIFT and about 2.2 mm for CenSurE and SURF. The average covariance factor for the targets-based method is 0.41 (below the acceptable threshold) and about two times worse for the detector-based method.

Regarding the result obtained for Test Site IV, the difference in the mean RMSE values are from -0.3 mm to 0.6 mm for all detectors, between detector-based and target-based methods. The average covariance for the target-based method is 0.46, which is two times lower than for the detector-based method. In the case of Test Site V, lower differences were obtained for affine detectors (values from 0.3 mm to 1.0 mm) than for detectors (2.2 mm to 4.1 mm). The covariance factor for the detector-based method is in the range of 0.83–0.99, and for the target-based is 0.72.

The inability to record all scans for Test Site VI was due

to the failure to identify suitable points for all detectors and affine detectors, except for ASIFT and AFAST. When assessing the RMSE values used, similar results were obtained from the pixels detected using the ASIFT detector and the target-based method. The accuracy was about 2–2.5 lower than that of the previously mentioned algorithms. The covariance coefficients obtained for the AFAST, ASIFT, and target-based methods were 0.91, 0.94 and 0.7, respectively.

The covariance factors for all test sites showed that the feature-based method yields a higher controllability of the points and their geometric distribution.

The study clearly shows that the registration accuracy depends on the quality of the point cloud effected by the TLS technique. The main relevant findings are presented below:

- The blob detectors, particularly SIFT, SURF and ASIFT, demonstrate improved orientation accuracies over the target-based method for the Test Sites (I and II) characterised by repeatable texture or similar texture and materials, for example, bricks. Furthermore, the acceptable results were presented by AFAST, ASURF, and ACenSurE (differences did not exceed 1.5 mm, and values did not exceed 3.4 mm).
- The results from Test Site III (featuring multiple architectural details) show that only with FAST, SIFT, BRISK, CenSurE, AFAST, and ASIFT detectors is the quality of registration higher than the target-based method. Meanwhile, ABRISK, SURF, and ASURF had RMSE values higher than 2 mm. Points detected by the ACenSurE detector did not allow for a correct registration.
- The results obtained at Test Site IV (room with wall paintings imitating a spatial effect without architectural details) indicate that all points and blob detectors allow for point cloud registration with the same accuracy as the target-based method.
- In the case of Test Site V (office room), with the scanner positions placed near walls, only affine detectors could obtain results similar to those of the target-based method. The RMSE for all coordinates is approximately 3 mm higher for all detectors than target-based method for other detectors.
- The highest RMSE values were obtained for Test Site VI (empty shopping mall) owing to the flat, textureless surfaces of the measured site and scanner position to perform a multi-station registration. Only the ASIFT and AFAST algorithms can perform a multi-station registration. However, a result similar to the target-based approach was obtained by the ASIFT method.
- For a complete and correct automatic point cloud registration with an accuracy similar to that of the target-based method, it is recommended that ASIFT or AFAST algorithms are used, because these detectors could perform a multi-station registration at any of the Test Sites.

Iterative Closest Points (ICP)

The second assessment of the accuracy of TLS registration based on "standard" and affine detectors was to compare with the results obtained using the point-to-point ICP method (implemented in open-source CloudCompare software). The point clouds were resampled to a fixed distance of 1 mm between points. The linear distance between pairs of point clouds was used to evaluate the accuracy of point cloud matching. Figures 13–18 show the results of the worst-case scenario for all test areas. Each figure contains 12 histograms showing the probability density function of linear deviations between point clouds using the target-based method, the ICP point-to-point, BRISK, CenSurE, FAST, SIFT, SURF, ABRISK, ACenSurE, AFAST, ASIFT, and ASURF.

An analysis of the shape of the probability density histogram of linear deviations (Figure 13) shows that for the results obtained using ASIFT, SIFT, ASURF, SURF, Target-based and ICP methods, the shape of the distribution approximately corresponds to a chi-square distribution. The shape of the probability density histogram of linear deviations for the CenSurE detector is flat, which means that the scan registration was performed incorrectly. The distributions do not take a chi-square shape when analysing the other histograms (for ABRISK, BRISK, ACenSurE, AFAST, and FAST). Yet, for 95% of the points, the distance does not exceed 6 mm (below the determined scanning resolution of 6 mm/10 m).

In the case of Test Site II (Figure 14), only for the target-based method and CenSurE was the distribution of deviations not comparable to the chi-square distribution. For the Target-based method and based on the points detected by the CenSurE algorithm for 95% of the points, the distance did not exceed 6 mm. The peak of the histogram of the probability density of linear deviations between the worst-registered pair of scans by the CenSurE detector was approximately 3 mm. For the CenSurE detector (the pair of scans registered that was worst registered), the histogram peak of probability density histogram of linear deviations equalled approximately 3 mm.

The analysis of the results shown in Figure 15 shows that for Test Site III, the smallest deviations between pairs of point clouds were obtained using the ICP method (Figure 15b). It should also be noted that the results obtained for detectors and affine detectors (Figure 15c– l) are similar for the target-based method (Figure 15a), and the peak of the histogram is approximately 2 mm.

Based on the analysis of the results for Test Site IV (Figure 16), the use of both state-of-the-art methods, i.e. target-based and ICP, as well as the SIFT, and SURF algorithms with their affine counterparts, allows for correct matching of point clouds, as evidenced by the distribution of chi-square liner deviations. When considering the results obtained for the other detectors, it should be noted that the scans were correctly registered despite not obtaining a chi-square distribution. This indicates that for 95% of the points, the distance does not exceed 6 mm, which does not exceed a scanning point resolution of 6 mm/10 m.

Evaluating the results obtained for Test Site V (Figure 17), an analogy can be drawn with the results obtained for Test Site IV. There were lowest linear deviations for affine detectors, especially for AFAST, ASIFT, and ASURF, than for "standard" detectors. This is particularly evident for the ASIFT detector, for which the distribution of linear deviations values assumes a chi-square distribution, and its shape is similar to the shapes of the linear deviation histograms used for state-of-the-art methods.

The analysis of the linear deviations histograms confirmed that the lowest accuracy of point cloud registration results were obtained for the target-based method (Figure 18a) and the highest accuracy for ICP (Figure 18b). The reason for the low accuracy of the point cloud registration is the resolution of the scan (12 mm/10 m), which translates into point cloud density and problems in identifying the centre of the mark with high accuracy. For this reason, the ICP method, which allows for the correct data orientation, is recommended. When considering the results obtained for affine detectors, it should be noted that, although the distribution of linear deviations is not similar to a chi-square distribution, the results of the registration of the pair of scans are acceptable, as they do not exceed the accepted scan resolution of 12 mm/10 m. In summary, the data registration results show that using the affine detector allows for a robust registration, and choosing the ASIFT detector allows for a full data registration.

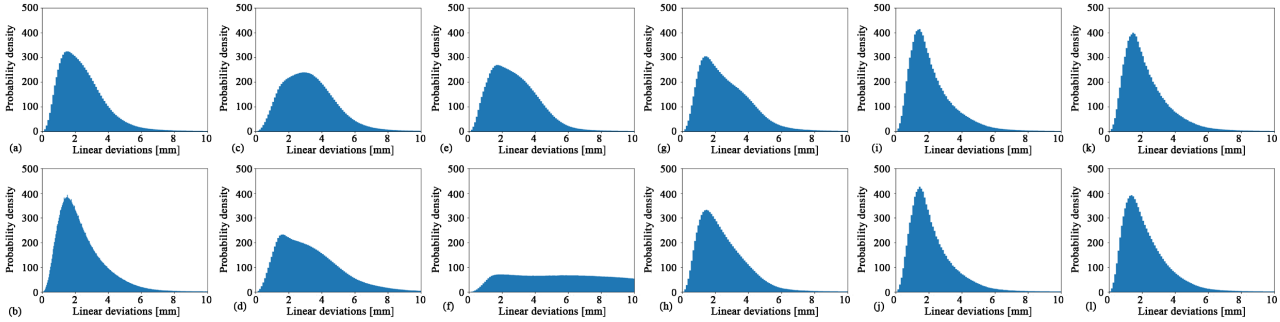

Figure 13. The probability density histogram of linear deviations between the worst oriented pair of scans for Test Site I: (a) Target-based method, (b) ICP point-to-point, (c) ABRISK, (d) BRISK, (e) ACenSurE, (f) CenSurE, (g) AFAST, (h) FAST, (i) ASIFT, (j) SIFT, (k) ASURF and (l) SURF

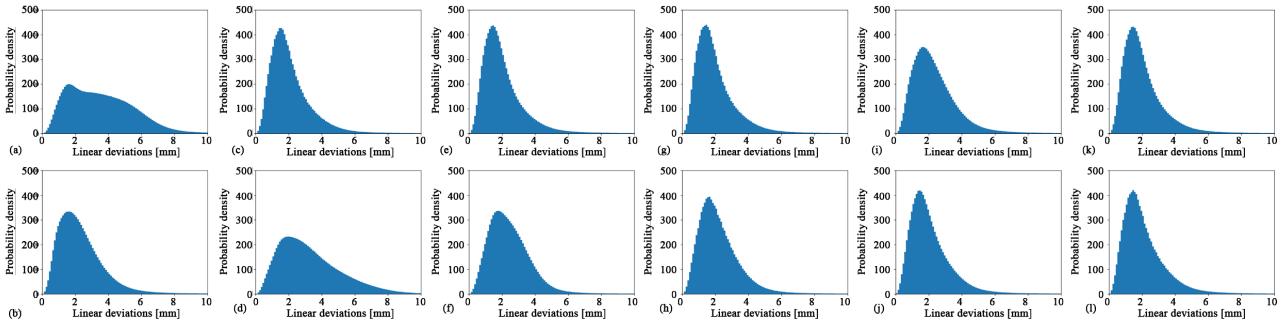

Figure 14. The probability density histogram of linear deviations between the worst oriented pair of scans for Test Site II: (a) Target-based method, (b) ICP point-to-point - CloudCompare, (c) ABRISK, (d) BRISK, (e) ACenSurE, (f) CenSurE, (g) AFAST, (h) FAST, (i) ASIFT, (j) SIFT, (k) ASURF, and (l) SURF

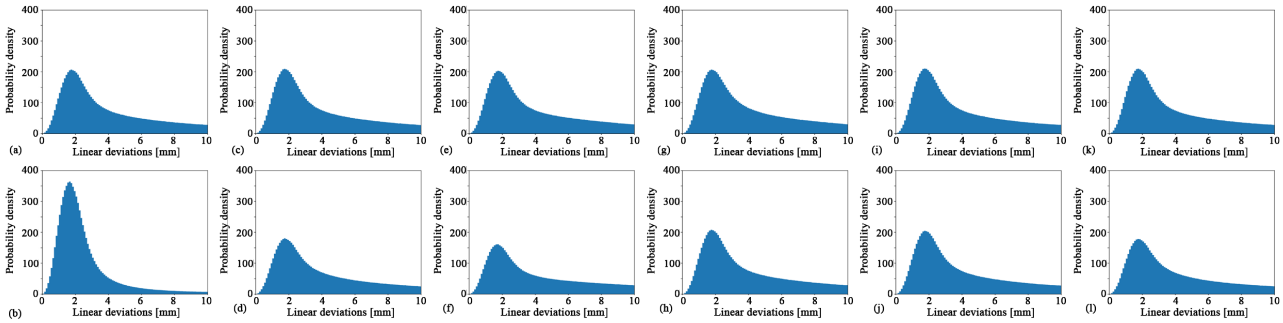

Figure 15. The probability density histogram of linear deviations between the worst oriented pair of scans for Test Site III: (a) Target-based method, (b) ICP point-to-point - CloudCompare, (c) ABRISK, (d) BRISK, (e) ACenSurE, (f) CenSurE, (g) AFAST, (h) FAST, (i) ASIFT, (j) SIFT, (k) ASURF, and (l) SURF

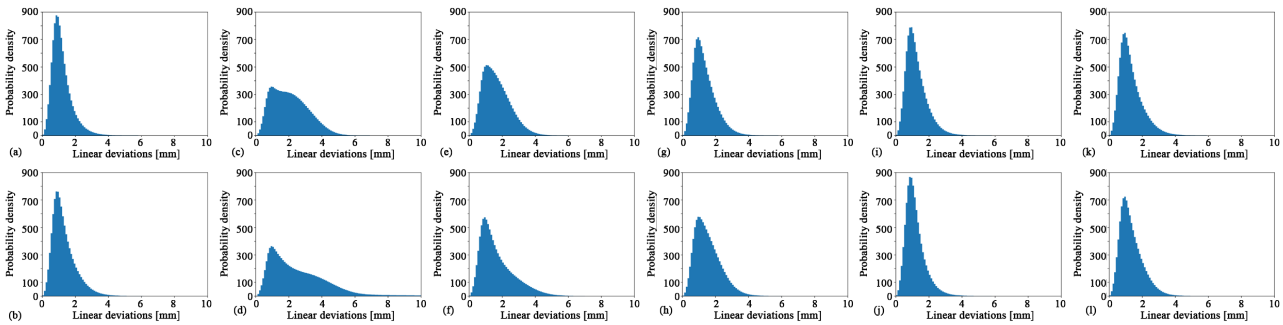

Figure 16. The probability density histogram of linear deviations between the worst oriented pair of scans for Test Site IV: (a) Target-based method, (b) ICP point-to-point – CloudCompare, (c) ABRISK, (d) BRISK, (e) ACenSurE, (f) CenSurE, (g) AFAST, (h) FAST, (i) ASIFT, (j) SIFT, (k) ASURF, and (l) SURF

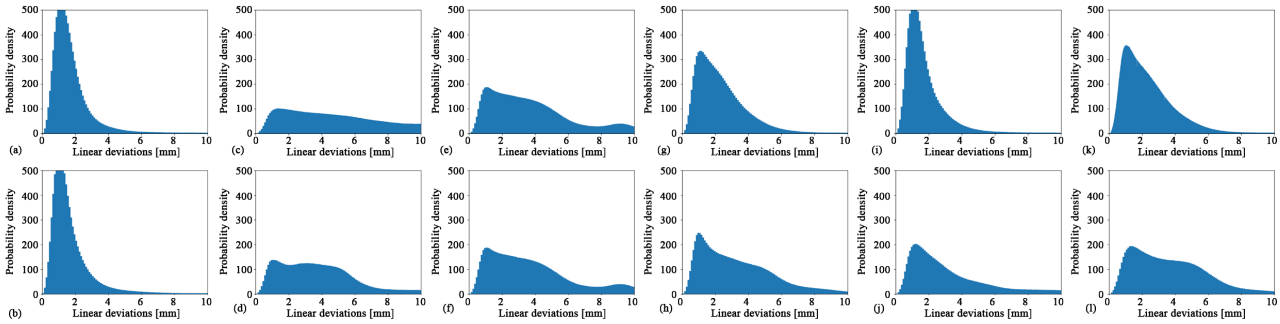

Figure 17. The probability density histogram of linear deviations between the worst oriented pair of scans for Test Site V: (a) Target-based method, (b) ICP point-to-point – CloudCompare, (c) ABRISK, (d) BRISK, (e) ACenSurE, (f) CenSurE, (g) AFAST, (h) FAST, (i) ASIFT, (j) SIFT, (k) ASURF, and (l) SURF

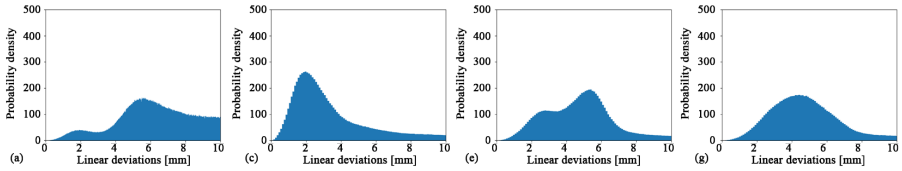

Figure 18. The probability density histogram of linear deviations between the worst oriented pair of scans for Test Site VI: (a) Target-based method, (b) ICP point-to-point – CloudCompare, (c) AFAST, and (d) ASIFT

The analysis of the overall time for TLS registration

The final comparative analysis compared the overall time for TLS registration using the proposed and state-of-the-art methods. The time taken to (1) convert point clouds from the scanner's native format to pts files, (2) convert point clouds to raster format, (3) import point clouds in pts format into CloudCompare software, (4) process time using feature-based TLS registration, and (5) using ICP and target-based methods was assessed. All calculations were performed on the CPU. The results are presented in Table 4.

Analysing the results presented in Table 4, it can be seen that converting raw point clouds to pts format depends on the number of point clouds being processed. It is a significant component in the overall TLS point cloud registration time. However, it should be emphasised that if data are processed in external software, this step is essential. When comparing the time required to convert point clouds to raster form with the time necessary to import point clouds into CloudCompare software (used to measure tie points using the target-based or ICP method), it might be seen that the times are similar, and the maximum difference for Test Site IV is 4 minutes and 40 seconds.

When comparing processing times using affine detectors and affine detectors, a significant difference in total processing time is noticeable. This is caused, as described in sections 4.2 and 4.3, by the search time for a single key point and the higher number of detected points. The analyses show that the shortest orientation time (disregarding the point cloud conversion time and raster generation) was obtained with the BRISK detector and the longest – with all test sites. Differences in TLS registration times depending on the detector used are also due to the specific test site. For Test Sites I and II (basements consisting of irregularly shaped brick and mortar structures with arch-shaped ceilings), the data processing time was the longest, as the algorithms mentioned above allowed the detection of a significantly higher number of points than for the other Test Sites (Figure 5), where these times are similar.

Comparing the feature-based registration method results with the target-based and ICP methods, it should be noted that (1) the shortest data fusion time was obtained using all detectors on Test Sites except the SURF and FAST detector on Test Site I.

Comparing the results for the feature-based registration method with the target-based and ICP methods, it might be seen that the results are close to each other except for the extreme cases: ASURF for all Test Sites, ASIFT and AFAST (Test Sites I and II).

To reduce the data processing time, it is possible to use a "standard" detector, remembering that it will require a supervised data analysis and selected cases of non-registration will require with the use of another registration method. To avoid the problem with TLS point cloud registration, it is worth using affine detectors and a fully automatic approach, although this can result (in selected cases) in significantly longer data processing time than using state-of-the-art methods.

5 Conclusion

The aim of this paper was to demonstrate the use of affine detectors in the TLS registration process to confirm that the use of a particular detector type is reflected in the accuracy and completeness of the registration process. To demonstrate this through a multi-stage TLS registration, blob and corner detectors were employed and affine detectors and point clouds converted to intensity spherical images. In order to assess the impact of the application of the affine parameter in the detectors, it was decided to use the VI Test Sites of the interiors of cultural heritage and public buildings located at the Royal Castle in Warsaw (Test Site I and II; characterised by a lack of decorative structures), Museum of King Jan III's Palace at Wilanów (Test Site III; having decorative elements, ornaments and materials on the walls), flat frescoes (Test Site IV), a narrow office (Test Site V) and a shopping mall (Test Site VI). The experiments demonstrated that:

- Point clouds are converted into the intensity raster, and detectors allow for a fully automatic TLS point cloud registration, regardless of the object's interior type.
- The selection of the detector should be determined by the object's interior type, characterised by a good texture, complex geometry, and the number of ornaments (such as cultural heritage sites); it is possible to use FAST, SURF, and

Table 4. The overall time for TLS point clouds registration

Test site	Data preprocessing Time [Minutes & Seconds] Conversion from RAW to PTS file	Conversion point clouds to raster data	Import point clouds to CloudCompare
I	38&12	17&48	14&05
II	57&18	26&42	26&24
III	74&11	17&22	17&00
IV	39&10	17&48	13&08
V	80&56	35&36	33&12
VI	70&21	31&09	30&58

Test site/ Detector	Feature-based TLS point cloud registration Time [Minutes & Seconds] BRISK	ABRISK	CenSurE	ACenSurE	FAST	AFAST	SIFT	ASIFT	SURF	ASURF
I	1&58	38&54	1&33	15&22	9&26	317&18	3&25	93&19	13&44	55&07
II	1&17	30&41	1&45	21&44	10&45	532&20	4&44	214&25	19&28	319&01
III	1&10	8&54	1&08	7&49	1&35	12&07	1&35	21&41	2&14	47&41
IV	1&36	9&33	1&37	9&57	1&41	13&12	1&38	20&07	4&26	82&50
V	1&14	16&45	1&19	18&06	1&30	19&51	1&10	32&59	4&04	84&40
VI	1&22	18&17	1&21	18&40	1&37	21&09	1&01	34&08	5&04	87&04

Test site	The current state-of-the-art registration methods Time [Minutes & Seconds] Target-based	ICP
I	8&28	12&36
II	13&16	11&08
III	9&43	19&07
IV	11&22	11&14
V	21&15	39&11
VI	18&34	19&46

SIFT detectors and their equivalents in the form of affine detectors. For TLS point clouds registration of textureless and uncomplicated geometry interiors (public buildings), such detectors as AFAST or ASIFT are recommended. Meanwhile, using the ASIFT detector makes it possible to record the point cloud regardless of the geometric relationship between the individual scans and the field under study.

- Adding affinity to detectors (affine detectors) allows for a significant increase in the accuracy of pair scans co-registration and completeness of pairs co-registration (Table. 3). There is a noticeable improvement in point cloud co-registration for the ACenSurE and ABRISK detectors for Test Site I-V. Using AFAST and ASIFT allows for multi-station registrations of all scans.
- The calculations of points detection time for "standard" detectors and affine detectors demonstrate that, on average, it takes longer to detect key points using point detectors than blob detectors. The smallest deviations in the ratio (affine detector to detector) were observed for the ASIFT and ASURF detectors. The single key points search time for the ASURF detector was shorter than the CenSurE and SIFT detectors.
- Using the affine detectors allows for extracting a high number of key points and increases the accuracy and completeness of the TLS registration process. The number of key points detected increased for point detectors (ABRISK and AFAST) by 8–12 times and for blob detectors (ACenSurE, ASURF and ASIFT) by about 10–24 times.
- When assessing the point clouds registration accuracy on signalised check points, the lower values can be observed for maximum RMSE errors for blob affine detectors than detectors and higher values – for corner detectors and affine detectors (not more than 4 mm in the extreme cases, typically 2 mm). The mean values for blob affine detectors and detectors are similar and lower for the FAST detector. When comparing the results obtained with the target-based registration method, it can be noted that they are similar (differences do not exceed in extreme situations 3.5 mm, typically less than 2 mm), which proves that the use of affine detectors for point cloud registration is appropriate and recommended.
- The key issue with point cloud registration is that it is robust to the occurrence of outliers in observations and can detect them easily through the so-called observational controllability. For this purpose, the so-called internal reliability indices are used, which allow for a rapid verification of the number and spatial distribution of points. It is assumed that in the case of low internal reliability indices, observations have relatively low controllability and, thus, low detection of outliers in the reference points. The target-based method challenges the distribution of numerous points, often proving it difficult or even unfeasible. Conversely, the feature-based approach facilitates the automatic detection of many points. A dense distribution of points across the surveyed object enables relative point control and correct outlier removal.
- Internal reliability indices are not commonly used for TLS point cloud registration. For this reason, using such an approach when filtering tie points detected using affine detectors allows for increased controllability of points and the detection of outliers in the dataset. In the experiment, this contributed to fulfilling the network's controllability condition and improving the geometric distribution of tie points for the minimum values (an increase from 0.05 to 0.63, where 0.5 is the acceptable threshold value). When comparing results from the detector-based method with the values derived from points identified using the target-based

method, it becomes evident that for Test Site I, the averages fell within the range of 0.91 to 0.99, contrasting with the target-based method's average of 0.67. Similarly, for Test Site II, the averages ranged from 0.90 to 0.99, while the target-based method yielded an average of 0.20. Test Site III exhibited average covariance factor values of 0.95, approximately 4.5 times higher than the target-based method (0.2).

- Conversely, for Test Site IV, the average covariance factor obtained through the target-based method stood at 0.41, below the acceptable threshold and roughly twice as inaccurate as the detector-based methods. In the context of Test Site V, covariance factors for the detector-based method spanned between 0.83 and 0.99, while for the target-based method, it rested at 0.72. Finally, for Test Site VI, covariance factors were reported as 0.91, 0.94, and 0.7 for AFAST, ASIFT, and the target-based method, respectively.
- Upon a comparison of these results with values obtained for the points detected with the target-based method, for Test Site I, the average was between 0.91 and 0.99, while for the target-based method, the average was 0.67. For Test Site II, the average was between 0.90 and 0.99, while for the target-based method, was average is 0.20. For Test Site III, the average covariance factor values (0.95) were about 4.5 times higher compared to the target-based method (0.2); for Test Site IV, the average covariance factors for the targets-based method was 0.41 (below the acceptable threshold) and about 2 times lower than from the detector-based method. In the case of Test Site V, the covariance factor for the detector-based method was in the range of 0.83–0.99, while for the target-based method, it was 0.72 and for Test Site VI, the covariance factors were 0.91, 0.94 and 0.7 for AFAST, ASIFT and target-based, respectively.
- This paper presents a robust point cloud registration method based on point clouds transformed into intensity rasters in spherical mapping and affine detectors. The analyses show that its application enables point cloud registration with an accuracy similar to state-of-the-art methods: target-based and ICP. However, according to the reliability theory, its advantage over the target-based method is the possibility of detecting more tie points automatically with a better spatial distribution and robustness. It should be emphasised that the presented affine detector-based method does not require any pre-assumptions regarding point cloud pre-registration, which are crucial in the case of the ICP method, as they clearly define the correctness of the final registration.

Further research plans are to test the method's performance with respect to outdoor point clouds and point clouds acquired from ToF scanners for different scanning distances and resolutions.

Acknowledgements

The research was funded by the Warsaw University of Technology within the Excellence Initiative: Research University (IDUB) programme (No. 1820/55/Z01/2021).

References

Abbate, E., Sammartano, G., and Spanò, A. (2019). Prospective upon multi-source urban scale data for 3D documentation and monitoring of urban legacies. *The International Archives of the Photogrammetry, Remote Sensing and Spatial Information Sciences*, XLII-2/W11:11–19, doi:10.5194/isprs-archives-xlii-2-w11-11-2019.

Agrawal, M., Konolige, K., and Blas, M. R. (2008). Censure: Center surround extremas for realtime feature detection and matching. In *European conference on computer vision*, pages 102–115. Springer, doi:10.1007/978-3-540-88693-8_8.

Arif, R. and Essa, K. (2017). Evolving techniques of documentation of a world heritage site in Lahore. *The International Archives of the Photogrammetry, Remote Sensing and Spatial Information Sciences*, XLII-2/W5:33–40, doi:10.5194/isprs-archives-xlii-2-w5-33-2017.

Bae, K.-H. and Lichti, D. D. (2008). A method for automated registration of unorganised point clouds. *ISPRS Journal of Photogrammetry and Remote Sensing*, 63(1):36–54, doi:10.1016/j.isprsjprs.2007.05.012.

Bay, H., Tuytelaars, T., and Van Gool, L. (2006). *SURF: Speeded Up Robust Features*, pages 404–417. Springer Berlin Heidelberg, doi:10.1007/11744023_32.

Bianco, S., Ciocca, G., and Marelli, D. (2018). Evaluating the performance of Structure from Motion pipelines. *Journal of Imaging*, 4(8):98, doi:10.3390/jimaging4080098.

Biber, P. and Straßer, W. (2003). The normal distributions transform: A new approach to laser scan matching. In *Proceedings 2003 IEEE/RSJ International Conference on Intelligent Robots and Systems (IROS 2003)(Cat. No. 03CH37453)*, volume 3, pages 2743–2748. IEEE, doi:10.1109/IROS.2003.1249285.

Boehler, W., Vicent, M. B., Marbs, A., et al. (2003). Investigating laser scanner accuracy. *The international archives of photogrammetry, remote sensing and spatial information sciences*, 34(Part 5):696–701.

Bosché, F. (2010). Automated recognition of 3D CAD model objects in laser scans and calculation of as-built dimensions for dimensional compliance control in construction. *Advanced Engineering Informatics*, 24(1):107–118, doi:10.1016/j.aei.2009.08.006.

Canny, J. (1986). A computational approach to edge detection. *IEEE Transactions on Pattern Analysis and Machine Intelligence*, PAMI-8(6):679–698, doi:10.1109/tpami.1986.4767851.

Chen, Y., Chen, Y., and Wang, G. (2019). Bundle adjustment revisited. doi:10.48550/ARXIV.1912.03858.

Cheng, L., Chen, S., Liu, X., Xu, H., Wu, Y., Li, M., and Chen, Y. (2018). Registration of laser scanning point clouds: A review. *Sensors*, 18(5):1641, doi:10.3390/s18051641.

Cloudcompare (2024). CloudCompare project. https://cloudcompare-org.danielgm.net/.

Das, A. and Waslander, S. L. (2012). Scan registration with multi-scale k-means normal distributions transform. In *2012 IEEE/RSJ International Conference on Intelligent Robots and Systems*. IEEE, doi:10.1109/iros.2012.6386185.

Dong, Z., Yang, B., Liang, F., Huang, R., and Scherer, S. (2018). Hierarchical registration of unordered TLS point clouds based on binary shape context descriptor. *ISPRS Journal of Photogrammetry and Remote Sensing*, 144:61–79, doi:10.1016/j.isprsjprs.2018.06.018.

Fischler, M. A. and Bolles, R. C. (1981). Random sample consensus: a paradigm for model fitting with applications to image analysis and automated cartography. *Communications of the ACM*, 24(6):381–395, doi:10.1145/358669.358692.

Giżyńska, J., Komorowska, E., and Kowalczyk, M. (2022). The comparison of photogrammetric and terrestrial laser scanning methods in the documentation of small cultural heritage object – case study. *Journal of Modern Technologies for Cultural Heritage Preservation*, 1(1), doi:10.33687/jmtchp.001.01.0013.

Guo, Y., Sohel, F., Bennamoun, M., Lu, M., and Wan, J. (2013). Rotational projection statistics for 3D local surface description and object recognition. *International Journal of Computer Vision*, 105(1):63–86, doi:10.1007/s11263-013-0627-y.

Harris, C. and Stephens, M. (1988). A combined corner and edge detector. In *Procedings of the Alvey Vision Conference 1988*,

AVC 1988. Alvey Vision Club, doi:10.5244/c.2.23.

Hekimoglu, S., Demirel, H., and Aydin, C. (2002). Reliability of the conventional deformation analysis methods for vertical networks. In *FIG XXII International Congress*, pages 1–13. International Federation of Surveyors Washington, DC.

Karwel, A. K. and Markiewicz, J. (2022). The methodology of the archival aerial image orientation based on the SfM method. *Sensors and Machine Learning Applications*, 1(2), doi:10.55627/smla.001.02.0015.

Łapiński, S. (2011). Method of network reliability analysis based on accuracy characteristics. *Reports on Geodesy*, 90(1):265–270.

Leutenegger, S., Chli, M., and Siegwart, R. Y. (2011). BRISK: Binary robust invariant scalable keypoints. In *2011 International Conference on Computer Vision*. IEEE, doi:10.1109/iccv.2011.6126542.

Lowe, D. (1999). Object recognition from local scale-invariant features. In *Proceedings of the Seventh IEEE International Conference on Computer Vision*. IEEE, doi:10.1109/iccv.1999.790410.

Lowe, D. G. (2004). Distinctive image features from scale-invariant keypoints. *International Journal of Computer Vision*, 60(2):91–110, doi:10.1023/b:visi.0000029664.99615.94.

Lu-Xingchang and Liu-Xianlin (2006). *Reconstruction of 3D Model Based on Laser Scanning*, pages 317–332. Springer Berlin Heidelberg, doi:10.1007/978-3-540-36998-1_25.

Markiewicz, J., Łapiński, S., Bocheńska, A., and Kot, P. (2021). The reliability assessment of the TLS registration methods – the case study of the Royal Castle in Warsaw. *The International Archives of the Photogrammetry, Remote Sensing and Spatial Information Sciences*, XLIII-B2-2021:855–861, doi:10.5194/isprs-archives-xliii-b2-2021-855-2021.

Markiewicz, J., Kot, P., Markiewicz, u., and Muradov, M. (2023). The evaluation of hand-crafted and learned-based features in Terrestrial Laser Scanning-Structure-from-Motion (TLS-SfM) indoor point cloud registration: the case study of cultural heritage objects and public interiors. *Heritage Science*, 11(1), doi:10.1186/s40494-023-01099-9.

Markiewicz, J. and Zawieska, D. (2019). The influence of the cartographic transformation of TLS data on the quality of the automatic registration. *Applied Sciences*, 9(3):509, doi:10.3390/app9030509.

Markiewicz, J. S. (2016). The use of computer vision algorithms for automatic orientation of Terrestrial Laser Scanning data. *ISPRS - International Archives of the Photogrammetry, Remote Sensing and Spatial Information Sciences*, XLI-B3:315–322, doi:10.5194/isprsarchives-xli-b3-315-2016.

Moisan, L. and Stival, B. (2004). A probabilistic criterion to detect rigid point matches between two images and estimate the fundamental matrix. *International Journal of Computer Vision*, 57(3):201–218, doi:10.1023/b:visi.0000013094.38752.54.

Moussa, W. (2014). *Integration of digital photogrammetry and terrestrial laser scanning for cultural heritage data recording*. PhD thesis, University Of Stuttgart, Germany.

Mukupa, W., Roberts, G. W., Hancock, C. M., and Al-Manasir, K. (2016). A review of the use of terrestrial laser scanning application for change detection and deformation monitoring of structures. *Survey Review*, pages 1–18, doi:10.1080/00396265.2015.1133039.

Muradov, M., Kot, P., Markiewicz, J., Łapiński, S., Tobiasz, A., Onisk, K., Shaw, A., Hashim, K., Zawieska, D., and Mohi-Ud-Din, G. (2022). Non-destructive system for in-wall moisture assessment of cultural heritage buildings. *Measurement*, 203:111930, doi:10.1016/j.measurement.2022.111930.

Nowak, E. and Odziemczyk, W. (2018). Adjustment of observation accuracy harmonisation parameters in optimising the network's reliability. *Reports on Geodesy and Geoinformatics*, 105(1):53–59, doi:10.2478/rgg-2018-0006.

Pavlov, A. L., Ovchinnikov, G. V., Derbyshev, D. Y., Tsetserukou, D., and Oseledets, I. V. (2017). AA-ICP: Iterative Closest Point with Anderson Acceleration. *2018 IEEE International Conference On Robotics And Automation (ICRA)*, doi:10.48550/ARXIV.1709.05479.

Pomerleau, F., Colas, F., and Siegwart, R. (2015). A review of point cloud registration algorithms for mobile robotics. *Foundations and Trends in Robotics*, 4(1):1–104, doi:10.1561/2300000035.

Prószyński, W. and Łapiński, S. (2018). Reliability analysis for non-distorting connection of engineering survey networks. *Survey Review*, 51(366):219–224, doi:10.1080/00396265.2018.1425605.

Rashidi, M., Mohammadi, M., Sadeghlou Kivi, S., Abdolvand, M. M., Truong-Hong, L., and Samali, B. (2020). A decade of modern bridge monitoring using Terrestrial Laser Scanning: Review and future directions. *Remote Sensing*, 12(22):3796, doi:10.3390/rs12223796.

Rofatto, V. F., Matsuoka, M. T., Klein, I., Veronez, M. R., Bonimani, M. L., and Lehmann, R. (2018). A half-century of baarda's concept of reliability: a review, new perspectives, and applications. *Survey Review*, 52(372):261–277, doi:10.1080/00396265.2018.1548118.

Rosten, E. and Drummond, T. (2006). *Machine Learning for High-Speed Corner Detection*, pages 430–443. Springer Berlin Heidelberg, doi:10.1007/11744023_34.

Salvi, J., Matabosch, C., Fofi, D., and Forest, J. (2007). A review of recent range image registration methods with accuracy evaluation. *Image and Vision computing*, 25(5):578–596, doi:10.1016/j.imavis.2006.05.012.

Staiger, R. (2005). The geometrical quality of Terrestrial Laser Scanner (TLS). In *Proceedings of FIG Working Week and GSDI-8, Cairo, Egypt*, pages 1–11.

Takeuchi, E. and Tsubouchi, T. (2006). A 3-D scan matching using improved 3-D normal distributions transform for mobile robotic mapping. In *2006 IEEE/RSJ International Conference on Intelligent Robots and Systems*. IEEE, doi:10.1109/iros.2006.282246.

Tam, G. K. L., Cheng, Z.-Q., Lai, Y.-K., Langbein, F. C., Liu, Y., Marshall, D., Martin, R. R., Sun, X.-F., and Rosin, P. L. (2013). Registration of 3D point clouds and meshes: A survey from rigid to nonrigid. *IEEE Transactions on Visualization and Computer Graphics*, 19(7):1199–1217, doi:10.1109/tvcg.2012.310.

Tazir, M. L., Gokhool, T., Checchin, P., Malaterre, L., and Trassoudaine, L. (2019). Cluster ICP: Towards sparse to dense registration. In *Intelligent Autonomous Systems 15. IAS 2018. Advances in Intelligent Systems and Computing*, volume 867, pages 730–747. Springer, doi:10.1007/978-3-030-01370-7_57.

Tobiasz, Markiewicz, Łapiński, Nikel, Kot, and Muradov (2019). Review of methods for documentation, management, and sustainability of cultural heritage. Case Study: Museum of King Jan III's Palace at Wilanów. *Sustainability*, 11(24):7046, doi:10.3390/su11247046.

Tola, E., Lepetit, V., and Fua, P. (2010). DAISY: An efficient dense descriptor applied to wide-baseline stereo. *IEEE Transactions on Pattern Analysis and Machine Intelligence*, 32(5):815–830, doi:10.1109/tpami.2009.77.

Tuytelaars, T. and Mikolajczyk, K. (2007). Local invariant feature detectors: A survey. *Foundations and Trends® in Computer Graphics and Vision*, 3(3):177–280, doi:10.1561/0600000017.

Urban, S. and Weinmann, M. (2015). Finding a good feature detector-descriptor combination for the 2D keypoint-

based registration of TLS point clouds. *ISPRS Annals of the Photogrammetry, Remote Sensing and Spatial Information Sciences*, II-3/W5:121–128, doi:10.5194/isprsannals-ii-3-w5-121-2015.

Vacca, G., Mistretta, F., Stochino, F., and Dessi, A. (2016). Terrestrial laser scanner for monitoring the deformations and the damages of buildings. *The International Archives of the Photogrammetry, Remote Sensing and Spatial Information Sciences*, XLI-B5:453–460, doi:10.5194/isprs-archives-xli-b5-453-2016.

Wang, W., Zhao, W., Huang, L., Vimarlund, V., and Wang, Z. (2014). Applications of terrestrial laser scanning for tunnels: a review. *Journal of Traffic and Transportation Engineering (English Edition)*, 1(5):325–337, doi:10.1016/s2095-7564(15)30279-8.

Weinmann, M. (2016). *From Irregularly Distributed 3D Points To Object Classes*. Reconstruction And Analysis Of 3D Scenes. Springer International Publishing, doi:10.1007/978-3-319-29246-5.

Wojtkowska, M., Kedzierski, M., and Delis, P. (2021). Validation of terrestrial laser scanning and artificial intelligence for measuring deformations of cultural heritage structures. *Measurement*, 167:108291, doi:10.1016/j.measurement.2020.108291.

Xu, Y., Boerner, R., Yao, W., Hoegner, L., and Stilla, U. (2019). Pairwise coarse registration of point clouds in urban scenes using voxel-based 4-planes congruent sets. *ISPRS Journal of Photogrammetry and Remote Sensing*, 151:106–123, doi:10.1016/j.isprsjprs.2019.02.015.

Yu, G. and Morel, J.-M. (2011). ASIFT: An algorithm for fully affine invariant comparison. *Image Processing On Line*, 1:11–38, doi:10.5201/ipol.2011.my-asift.

Z+F (2024). Zoller + Fröhlich. https://www.zofre.de/en/.